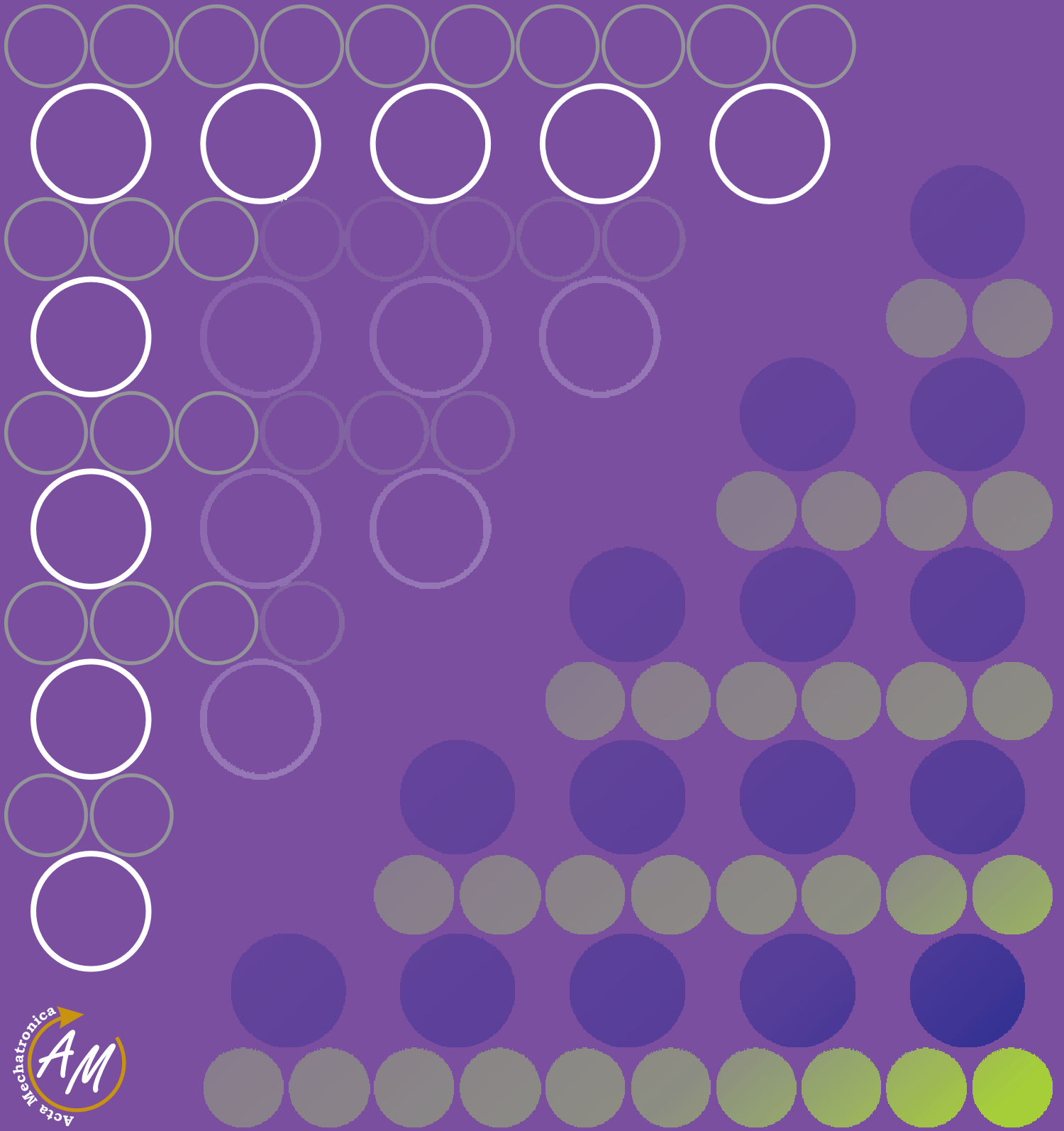


ACTA MECHATRONICA

2019 Volume 4

Issue 4



International Scientific Journal about Mechatronics
electronic journal
ISSN 2453-7306

CONTENTS
(DECEMBER 2019)

(pages 1-4)

**CONTACTLESS PROTECTIVE DEVICES FOR DEPLOYMENT
IN AUTOMATED WORKPLACES**

Marek Vagaš, Alena Galajdová, Dušan Šimšík

(pages 5-10)

**EXPERIMENTAL VERIFICATION OF OBJECT LEVITATION
BY OPTICAL SENSOR**

Erik Prada, Ivan Virgala, Martin Varga

(pages 11-15)

ADAPTABLE MOBILE ROBOT FOR ROUGH TERRAIN

Michal Kelemen, Filip Filakovský, Peter Ferenčík

(pages 17-21)

AIRFLOW MEASUREMENT TEST DEVICE FOR AIRFLOW SENSORS

Tatiana Kelemenová

(pages 23-28)

GLUED JOINTS IN THE AUTOMOTIVE INDUSTRY

Silvia Maláková, Anna Guzanová, Peter Frankovský, Vojtech Neumann, Erik Janoško

(pages 29-34)

EVALUATION OF RESIDUAL STRESSES USING OPTICAL METHODS

Ján Kostka, Peter Frankovský, Peter Čarák, Vojtech Neumann

doi:10.22306/am.v4i4.49

CONTACTLESS PROTECTIVE DEVICES FOR DEPLOYMENT IN AUTOMATED WORKPLACES

Marek Vagaš

Technical University of Kosice, Faculty of Mechanical Engineering, Letna 9, Kosice, Slovak Republic,
marek.vagas@tuke.sk (corresponding author)

Alena Galajdová

Technical University of Kosice, Faculty of Mechanical Engineering, Letna 9, Kosice, Slovak Republic,
alena.galajdova@tuke.sk

Dušan Šimšík

Technical University of Kosice, Faculty of Mechanical Engineering, Letna 9, Kosice, Slovak Republic,
dusan.simsik@tuke.sk

Keywords: light curtains, automation, human protection

Abstract: Safety in automated workplaces is the most important feature of any machine, equipment and system as a whole in a modern and advanced society, where some part of it performs mechanical movement. The task is a set of comprehensive measures to prevent contact / collision of the device (robot, conveyor etc.) during this movement with any part of human operator. In addition, behaviour of modern automated workplaces is not always predictable, since movement (performed inside the automated cell) are usually controlled by a control program whose structure is only known to the manufacturer's programmer. These reasons pointed to the advanced functions use that is available in such equipment as light curtains.

1 Introduction

Light curtains as an element for implementation in automated workplaces usually serves as command at workplace to stop before operator is at risk position. This type of device can protect large areas. The advantage over mechanical covers lays in free access to the automated workplace, shorter setup time, material loading and so on. Protective devices must detect persons, parts of the body or objects reaching into the danger zone. Entry between protected zone and danger zone shall not be permitted. If necessary, additional protective devices must be installed. Light curtains must be installed at a distance such that hazard ends before the person enters into the danger zone [1].

The light curtains are made in a version for scanning body parts or even of a whole person. Many versions are capable to identifying whether an operator is intruding into danger zone with its body or is entering supplying material for processing. We can say that it is a kind of "mechanical" equivalent to safety of electrical equipment, where it is necessary to protect human operators from danger before electric current. While requirements for providing of electrical safety are generally understood and considered to be very important, safety against mechanical movements of machines, robotic arms or other types of equipment has been neglected quite often for quite some time, although it can cause as serious accidents as e.g. electric shock [2].

In general, light curtains belong to the basic surface-mounted optical security sensors to ensure automatic protection of inputs and outputs to / from danger area that cannot be fitted with any other type of mechanical barrier (e.g. mechanical barrier, other type of barriers, etc.). This is especially in cases, when operator necessarily moves into the hazardous area and needs free entry and exit for reasons such as automatic supply or removal of finished parts, products and materials see figure 1.

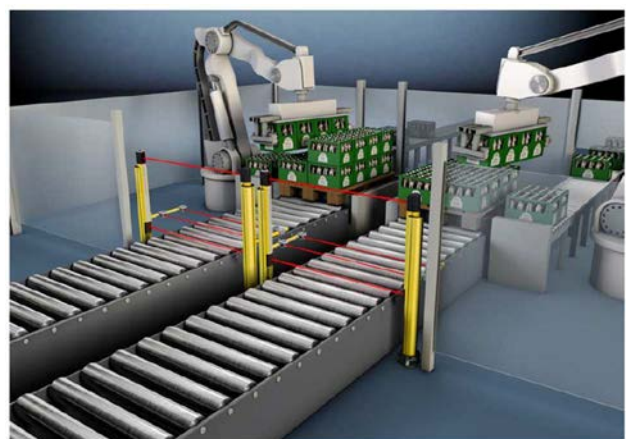


Figure 1 Example of light curtains installation into the automated workplace

As a typical good example is a mechanical safety fence or plexus-glass fences around a robotic loading station, where on the one hand it is necessary to ensure the entry

(arrival) of packaged products as well as the entry (delivery) of packaging material (e.g. pallets, boxes, etc.) and on the other hand, provide the exit (output) of filled packages on conveyor outside from the danger zone, e.g. for purpose of carrying or transporting by hand pallet truck or forklift truck [3]. In these cases, it is usually not possible to ensure mechanical securing of inputs and outputs by means of a classical mechanical door, even if the opening would be solved by its automatic opening. Not only because of high transport capacity for products on conveyors, or because of unwanted frequent shutdown of machine (in this case an industrial robot) to a safe state that significantly reduces machine life, but also because required by a human operator to check security from entire protected area [4]. It must be ensured that after closing of the door, there is no longer any person in danger zone.

2 Suitable position for assembly

Safety light curtains are installed in one of the following modes, see figure 2.

- Vertical (perpendicular to ground or at an angle greater than 30° up to 90°).
- Horizontal (horizontally to ground or at an angle approaching to 30°) to detect presence of a person in a hazardous area.
- Slant (assembly at an angle around 30°) for special functions simultaneously detecting vertical and horizontal entry under certain conditions.

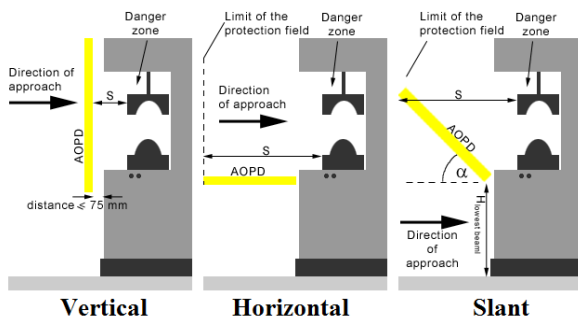


Figure 2 Positions for assembly of light curtain

2.1 Principle of light curtain

Light curtain design must be constructed in such a way that it does not cause injuries to the operator and prevents speculative starting of the automatic mode of workplace [5]. Usually, light curtain consists of receiver and transmitter units and protecting field is between them, see figure 3.

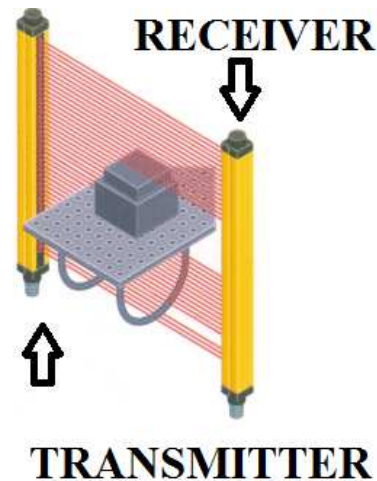


Figure 3 Principle of light curtain

Transmitting unit is equipped by source of infrared light that is transmitted in certain cycles to photo sensors in opposite part of barrier. In case of some object enter into the field and at least one line is missing, opposite receiver doesn't get information and generate signal about this situation, eventually it stop connected equipment resp. move equipment outside from this field (zone) [6]. Width of protected field is depended on maximum distance between transmit and receive unit for safe operation. Obviously starts from zero to several meters. High of protected field is depended only at unit's construction aspect, basically is limited to the two meters. Spacing of two neighbour lines determines resolution of equipment and its effectiveness. If the spacing is too small, it is very good for protection, because smaller object is matched. Resolution of equipment also determines a required IP.

2.2 Advanced function of light curtain

The most appropriate option for deployment of light curtain is using of so-called safety light curtains, equipped with function "muting". This function ensures guarding of free entrance space into the fence by detecting of unwanted entry by person, but at the same time allows completely automatic, i.e. without operator intervention, product entry or its exit [7].

This light curtain with flat surfaces allows detection by interruption (screening) of its rays with aim to control entry of a person into the danger zone, while temporary "muting function" that are implemented as in form of additional sensors allows correct detection / evaluation of the object arrival and automatic momentary deflection for (unlocking) equipment only during entry or exit of desired item [8]. At the same time, correct setting of "muting" function ensures that this unlocking does not cause a person to enter, but only by required products and required objects of automated workplace.

3 Trends – LEUZE MLD light curtain

Light curtains type MLD belongs to the basic curtains with flat surfaces detection by two or four safety sensors (according to the standard EN IEC 61496) at LEUZE electronic GmbH company, that regarding to the safety category 2, 3 or 4 and performance level PL (d, e – standard EN ISO 13849) realise variants with two or three ray system for sensing of input / output for area considered as dangerous. Obviously it is realised by separate active transmitter on one side and an active receiver (we note that active means electrically powered), or only with an active transceiver on the one hand and only a passive light reflecting the "pillar" on the other [9].

The passive reflector is not made up of a simple mirror type that reflects light ray from transmitter back to the receiver, but as a special set of two prisms that receive transmitted ray at one horizontal height level and send ray at the second horizontal height level to the receiver. In this way, required dual-ray horizontal – "optical network" is effectively created with help of single transmitter and receiver, see figure 4.

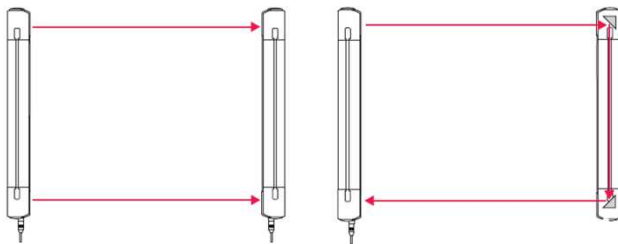


Figure 4 Separated receiver with transmitter (left) versus compound receiver with transmission solution (right)

"Muting" function requires presence of built-in control logic directly in the curtains MLD type (it is not necessary to use advanced safety relay or PLC) together with connection at MLD curtains, which attach in the opposite direction to the direction of movement of rays, in perpendicular to the rays of MLDs themselves. Their signal for sequential or simultaneous occultation by connecting to the related input of main MLD curtain provides information to control logic whether it will deny safety function of vertical rays (if it is desired object and safety outputs will not be activated or not).

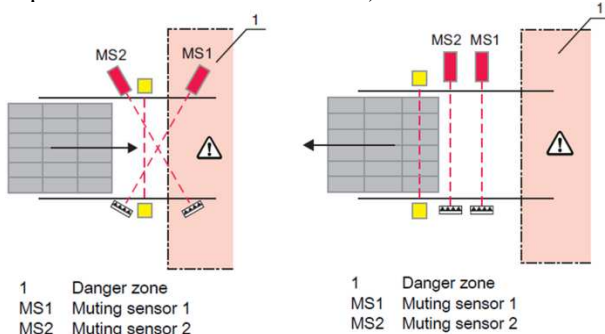


Figure 5 Principle of "muting" function

In particular, MLD 330 or MLD 530 design provides above-mentioned "muting" function, in addition to the vertical curtains themselves, by a set of two or four "muting" sensors (depending on the particular safety situation or selected function mode) that is supplied. Basic two modes of light curtains "muting" function can be seen at figure 5.

3.1 Example of MLD530-RT2M light curtain use

Example of MLD530-RT2M light curtain, their functionality and "muting" function is introduced at figure 6. This example consists of kit: MLDSET-M002-UDC-1600-S2, which contains 2 pieces of "muting" sensors with reflectors on four parts and also 2 pieces of fixing columns to the floor with its sophisticated attachment. This solution greatly simplifies correct installation and commissioning (easy adjustment of perpendicular position and relative rotation of columns by means of locking screws and integrated level) [10].

Kit MLD530-RT2M can also be ordered separately without columns and attached to our own vertical frame or column construction. The designation RT2M means that it is a version with active transceiver on one side and a passive reflective part on the opposite side of guarded vertical space. Their big advantage lay in complete wiring of electrical cables to only one side of guarded area and thus serves as a great simplification of electrical installation [11].

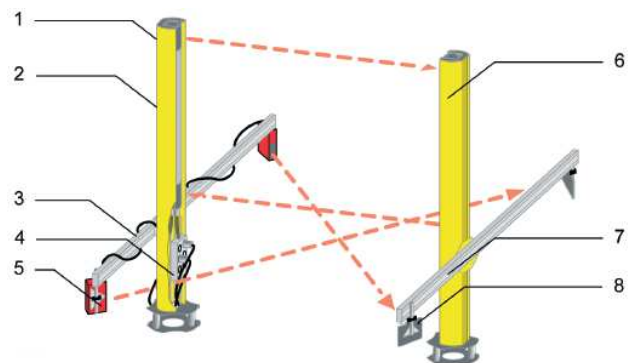


Figure 6 MLD530-RT2M light curtain kit

Where

- 1 = transceiver (associated transmitter/receiver),
- 2 = supporting column,
- 3 = locking "muting" arms with sensors,
- 4 = local interconnection terminal,
- 5 = "muting" sensor,
- 6 = passive reflection column,
- 7 = arms of "muting" reflectors,
- 8 = reflectors.

CONTACTLESS PROTECTIVE DEVICES FOR DEPLOYMENT IN AUTOMATED WORKPLACES

Marek Vagaš; Alena Galajdová; Dušan Šimšík;

4 Conclusion

We can state that advanced safety light curtains are reliably and cost-effectively protection against access into hazardous points and areas of automated workplaces. Suitable choice of the proposed variant together with different equipment functions that can be integrated or can be selected via safe control solutions is considered for replacing of traditional methods such is mechanical barriers, sliding gates and pull-back restraints. The range from small and compact types to extremely robust and resistant variants that withstand special ambient conditions up to the highest safety level makes them suitable for intuitive and cost-effective safely solution.

Acknowledgement

This work has been supported by the Slovak Grant VEGA 1/0330/19 - Research and design of algorithms and systems for the fusion of heterogeneous data in multisensor architectures and H2020: Manufacturing Industry Digital Innovation Hubs (MIDIH), reference no. 767498.

References

- [1] VAGAŠ, M.: Increasing of operational safety robotized workplaces by sensor equipment, *Global management and economics*, Vol. 2015, No. 1, pp. 158-162.
- [2] VAGAŠ, M., ŠIMŠÍK, D., ONOFREJOVÁ, D.: *Factors for successfully implementation of automated solutions based on industry 4.0*, ARTEP 2019 Automatizácia a riadenie v teórii a praxi, 13. ročník konferencie odborníkov z univerzít, vysokých škôl a praxe. Košice, Slovensko, Technická univerzita v Košiciach, pp. 1-8, 2019.
- [3] Details about light curtains, Online, Available: <https://www.schmachtl.cz/>, 2019.
- [4] FLEISCHAUER, H.: *Machine safety, Prevention of mechanical hazards*, Institut de recherche Robert-Sauvé en santé et en sécurité du travail (IRSST) et Commission de la santé et de la sécurité du travail du Québec (CSST), GUIDE RG-597, 2009.
- [5] PAWAR, V. M., LAW, J., MAPLE, C.: *Manufacturing Robotics, the next robotic industrial revolution*, UK-RAS White papers, UK-RAS Network, Robotics & Autonomous systems, 2016.
- [6] VAGAŠ, M., ŠIMŠÍK, D., GALAJDOVÁ, A., ONOFREJOVÁ, D.: *Safety as necessary aspect of automated systems*, ICETA 2018, Proceedings, 16th IEEE International Conference on Emerging eLearning Technologies and Applications, New Jersey (USA), Institute of Electrical and Electronics Engineers, pp. 617-622, 2018.
- [7] VRÁBEL, R., ABAS, M., TANUŠKA, P., VAŽAN, P., KEBÍSEK, M., ELIÁŠ, M., ŠUTOVÁ, Z., PAVLIAK, D.: *Mathematical approach to security risk assessment. Mathematical Problems in Engineering*, Vol. 2015, pp. 1-11, 2015. doi:10.1155/2015/417597
- [8] INABA, Y., SAKAKIBARA, S.: *Industrial intelligent robots in Springer handbook of automation 2009*, Part C, pp. 349-363, 2009.
- [9] BICCHI, A., PESHKIN, M. A., EDWARD COLGATE, J.: *Safety for Physical Human-Robot Interaction*, Springer Handbook of Robotics (Siciliano, B., Khatib, O.), Springer, Berlin, 2008.
- [10] CONSIGLIO, S., SELIGER, G., WEINERT, N.: *Development of Hybrid Assembly Workplaces, CIRP Annals*, Vol. 56, No. 1, pp. 37-40, 2007.
- [11] Daily Automation, *Vedecko-odborný recenzovaný internetový časopis. EN ISO 10218 – Priemyselné roboty a ich integrácia do priemyslu*, ISSN 2453-8175. (Original in Slovak)

Review process

Single-blind peer review process.

doi:10.22306/am.v4i4.50

EXPERIMENTAL VERIFICATION OF OBJECT LEVITATION BY OPTICAL SENSOR

Erik Prada

Technical University of Kosice, Faculty of Mechanical Engineering, Letna 9, Kosice, Slovak Republic, EU,
erik.prada@tuke.sk (corresponding author)

Ivan Virgala

Technical University of Kosice, Faculty of Mechanical Engineering, Letna 9, Kosice, Slovak Republic, EU,
ivan.virgala@tuke.sk

Martin Varga

Technical University of Kosice, Faculty of Mechanical Engineering, Letna 9, Kosice, Slovak Republic, EU,
martin.varga.2@tuke.sk

Keywords: magnetic levitation; optical sensor; laser module; motion detection

Abstract: Magnetic levitation used in technical applications such as transport systems in particular high-speed trains requires position control of the levitation system. It is precisely by suitable position control that there are no hazardous situations of contact of the mechanical parts outside the magnetic cushion, which can cause a dangerous state at very high speeds. However, for correct regulation, it is necessary to first turn out a reliable position sensing subsystem. It is precisely sensing the position using the optical method that this work is devoted to. The method of shielding is verified, when a smaller collimated beam falls on the photodiode. In order to measure the changes as accurately as possible, a laser collimating beam of light was chosen as the source.

1 Introduction

Magnetic levitation has a large perspective in practice, but the widespread use of this technology is not as enormous as some other technologies. The best-known application of magnetic levitation is the use of maglev trains, but it is not the only application of magnetic levitation in practice. To meet the functional model of magnetic levitation in practice is quite problematic in our latitudes. Germany is one of the few countries dedicated to magnetic levitation technology and has a high reputation worldwide with its Transrapid train (Figure 1). However, Germany is not the only country engaged in the practical application of magnetic levitation technology. Japan has an equally strong and possibly stronger presence in this industry. While the Germans focused on one development type of Transrapid, two different types of maglevs are being constructed in Japan, working on the HSST system and the Yamanashi system. The German Transrapid train and the Japanese HSST train operate on a similar motion system of an induction linear motor, where the stationary rotor consists of an aluminium reaction pad located at the top of the track. Three-phase stator coils are placed on the lower parts of the train, creating a magnetic field. The magnetic field make train levitation and the action of the traction force induced reaction to aluminium backing gives the train moving along magnetic wave.

Incorrect positioning of the levitating train from the ground could cause a train accident in the event of unexpected events occurring during operation. For this reason, sensing the position of the levitating object is an important part for regulation needs. However, in order to

design the necessary control, it is necessary to experimentally verify the position sensing by means of the optical shadow method [1-10].

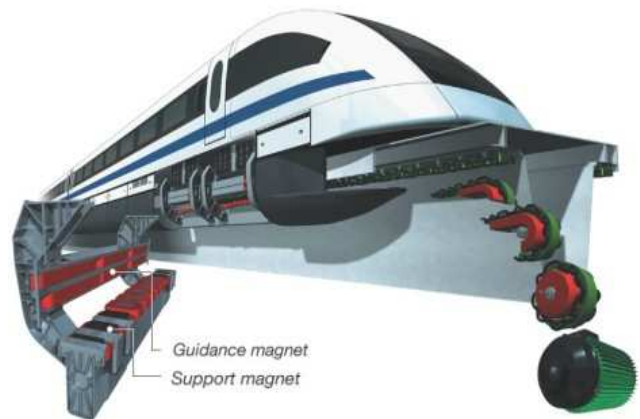


Figure 1 Transrapid train and its LIM system

1.1 Shadow method of measuring position

Magnetic levitation has a large perspective in practice, but the widespread use of this technology is not as enormous as some other technologies. The measurement of the position of the levitating object using the shadow method is based on the measurement of the current depending on the intensity of the incident light beam on the photosensitive sensor. The drop shadow on the photodiode will cause us to drop the current. Classic light or intense laser light can be used as the light beam source. The sensing unit thus consists of an emitter and an emitted beam sensor. It is most ideal to use a laser beam source as

EXPERIMENTAL VERIFICATION OF OBJECT LEVITATION BY OPTICAL SENSOR

Erik Prada; Ivan Virgala; Martin Varga

the emitter, the intensity of which is better reflected in the photodiode in a way of greater variance of the measured values. The figure (Figure 2) shows a diagram of the construction of the sensing. When designing it is appropriate to use a collimator, which provides us collimated beam.

The figure description:

1. coil
2. levitating object
3. photodiode
4. laser module with collimator
5. collimated laser beam

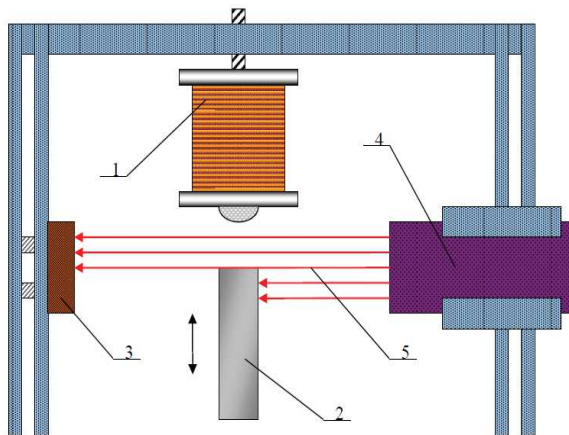


Figure 2 Schematic representation of the position sensing solution by the shadow method [2]

2 Experimental verification of the shadow method

The absolute measurement method was used for experimental verification. The aim of the measurement was experimental verification of the proposed solution. The experiment was performed under different conditions and settings and was therefore divided into several phases. The determined dependency characteristic is therefore different for each phase.

In the experiment we used LASER BTL 2000, LED light and Tesla 1PP75 photodiode. The BTL 2000 laser is primarily intended for medical use. Its positive feature is the great variability of possible settings. Negative can be considered the divergence of the radiated beam, whose angle was 36° . The active surface of the Tesla 1PP75 photodiode is 3.5 mm x 5.5 mm.

Current measurement was performed on a HP 34401A professional laboratory multimeter. The experiment was carried out on a rack set, on which the Laser BTL 2000 probe was mounted and compared to the photodiode Tesla 1PP75. The casting of the shadow on the photodiode was obtained using a metal sheet that was mounted in a rack with micrometres movement in the X-axis and Y-axis

directions. Schematic representation of the measurement is in the figure (Figure 3).

Description of measurement scheme:

1. Laser module holder
2. Laser module
3. photodiode
4. Stand with micrometre movement
5. Metal shielding plate
6. photodiode holder
7. ammeter

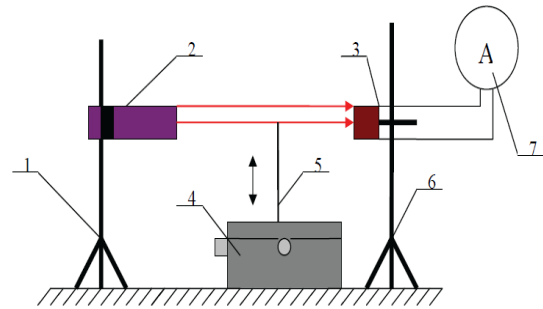


Figure 3 Scheme of current measurement by laser beam on photodiode [2]

Measurement procedure:

- connecting the laser to the mains, attaching the laser probe to the stand and connecting the photodiode through the wires to the multimeter input,
- turning on the laser and checking the beam so that it hits the sensor,
- setting the distance of the sensor from the laser module as required,
- grasping the shielding plate in a micrometres feed rack,
- zero setting of the shielding plate,
- turning on the multimeter and setting the DC current mode,
- recording the generated background currents of the measuring room,
- reading the value from the multimeter with zero cover,
- turn the screw to change the position of the shielding plate in 0.5 mm increments until the entire 10 mm interval has passed.
- reading three values from the multimeter every half millimetre and writing to the table,
- calculation of averages from the measured values and subsequent correction for total measurement error,
- Interpolation graphs [4].

Experimental verification consisted of three phases of measurement when the laser beam conditions changed [4].

For experimental phase I, we determined the following measurement conditions:

- Daylight measurements,
- continuous laser beam,
- laser beam power 8 mW,
- distance of probe from photodiode 100 mm.

EXPERIMENTAL VERIFICATION OF OBJECT LEVITATION BY OPTICAL SENSOR

Erik Prada; Ivan Virgala; Martin Varga

For experimental phase II we determined the following measurement conditions:

- Daylight measurements,
- 990 Hz pulsed laser beam,
- laser beam power 8 mW,
- distance of probe from photodiode 100 mm.

For experimental phase III, we determined the following measurement conditions:

- Daylight measurements,
- 500 Hz pulsed laser beam,
- laser beam power 8 mW,
- distance of probe from photodiode 100 mm.

3 Results of measuring position

The measured values were averaged and then corrected for the measurement error using the formula (2). The correction of the measured values (Table 1) consisted of subtracting the measurement error from the averaged value. We used the formula (1) to calculate the measurement error.

$$\delta_i = \delta_{REi} + \delta_{RAi} = [(0,01\% \times I_{xi}) + (0,004\% \times 100)] \quad (1)$$

$$I_{xKORi} = I_{xi} - \delta_i \quad (2)$$

3.1 Results of experimental phase I

The calculated values of the corrected current (Table 1) of the first experimental phase were shown as polynomial dependence in the (Figure 4), described by formulas (3), (4).

Table 1 Errors and correct values of the phase I - measurement process [4]

	1.	2.	3.	4.
δ_i [mA]	0,01104	0,01094	0,01092	0,01078
I_{xKOR} [mA]	70,39	69,39	69,19	67,79
	5.	6.	7.	8.
δ_i [mA]	0,00948	0,00814	0,00678	0,00567
I_{xKOR} [mA]	54,79	41,39	27,79	16,69
	9.	10.	11.	12.
δ_i [mA]	0,00432	0,00412	0,0041	0,0041
I_{xKOR} [mA]	3,12	1,19	0,99	0,99
	13.	14.	15.	16.
δ_i [mA]	0,00408	0,00408	0,00407	0,00407
I_{xKOR} [mA]	0,79	0,79	0,69	0,69
	17.	18.	19.	20.
δ_i [mA]	0,00406	0,00407	0,00407	0,00407
I_{xKOR} [mA]	0,59	0,69	0,69	0,69

$$y = 0,0023x^6 - 0,0459x^5 + 0,1115x^4 + 2,9304x^3 - 19,928x^2 + 20,255x + 68,064 \quad (3)$$

$$R^2 = 0,9928 \quad (4)$$

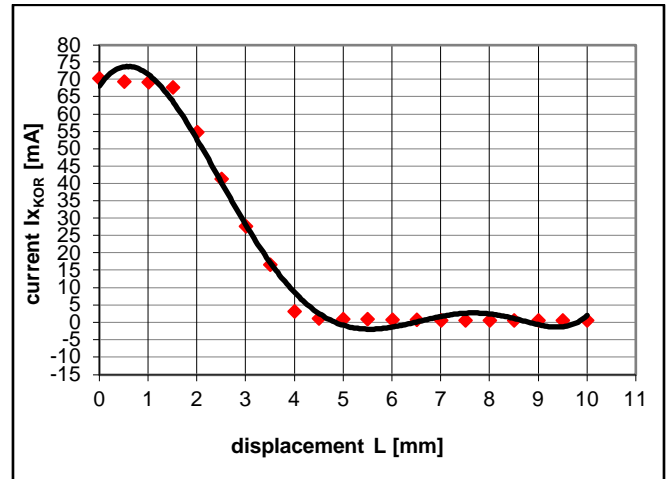


Figure 4 Graph of interpolation of corrected current versus cover length - phase I [2]

Since in our case we are mainly interested in the linear course of the graph because of the correct positioning and then the subsequent coil regulation, we focus mainly on the values forming the most linear parts of the graph. The shape of the graph is in the (Figure 5) and the interpolation equation is attached.

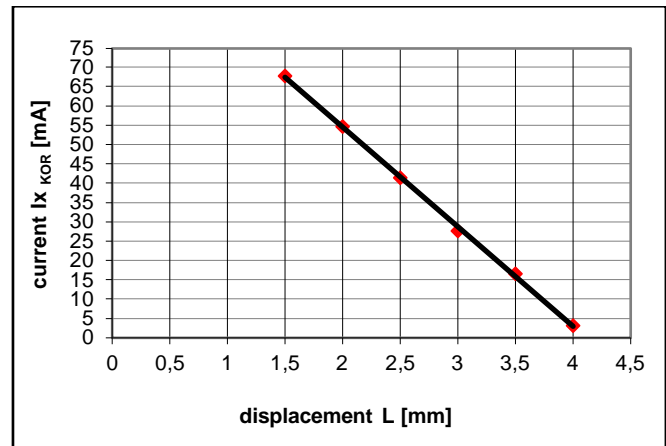


Figure 5 Graph of linear interpolation of selected work area values of phase I [2]

$$y = -25,786x + 106,17 \quad (5)$$

$$R^2 = 0,999 \quad (6)$$

3.2 Results of experimental phase II

The calculated values of the corrected current (Table 2) of the second experimental phase were shown as the polynomial dependence in the (Figure 6), described by formulas (7), (8).

EXPERIMENTAL VERIFICATION OF OBJECT LEVITATION BY OPTICAL SENSOR

Erik Prada; Ivan Virgala; Martin Varga

Table 2 Errors and correct values of the phase II - measurement process [4]

	1.	2.	3.	4.
δ_i [mA]	0,00869	0,00871	0,00881	0,00875
IxKOR [mA]	46,89	47,09	48,09	47,49
	5.	6.	7.	8.
δ_i [mA]	0,00875	0,00872	0,00820	0,00729
IxKOR [mA]	47,49	47,19	41,99	32,89
	9.	10.	11.	12.
δ_i [mA]	0,00628	0,00535	0,00449	0,00418
IxKOR [mA]	22,79	13,49	4,89	1,79
	13.	14.	15.	16.
δ_i [mA]	0,00419	0,00414	0,00413	0,00412
IxKOR [mA]	1,89	1,39	1,29	1,19
	17.	18.	19.	20.
δ_i [mA]	0,00412	0,00412	0,00412	0,00411
IxKOR [mA]	1,19	1,19	1,19	1,09

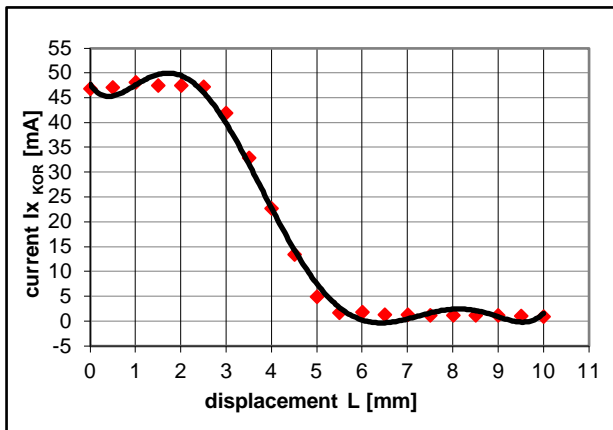


Figure 6 Graph of interpolation of corrected current versus cover length - phase II [2]

$$y = 0,0065x^6 - 0,2038x^5 + 2,3622x^4 - 11,953x^3 + 23,275x^2 - 13,702x + 47,685 \quad (7)$$

$$R^2 = 0,9955 \quad (8)$$

In the second experimental phase we were also interested in the linear part of the graph, because of the correct positioning and then the coil regulation. The shape of the graph is in the figure (Figure 7). It can be seen that the values obtained from the pulsed laser are almost completely linear and therefore this linearity can also be used for positioning. During this phase, the linear character values start at 2 mm and end at 5.5 mm.

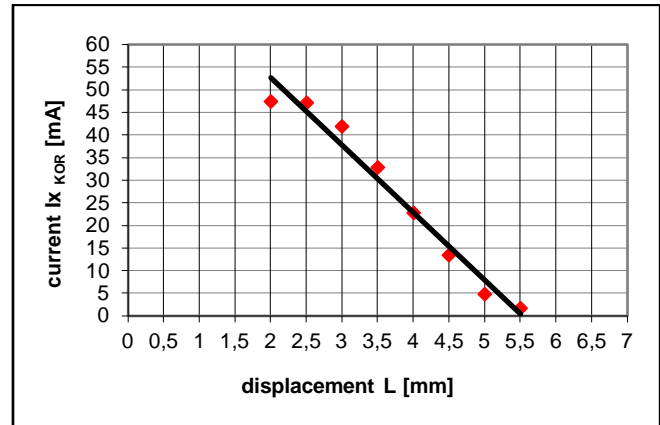


Figure 7 Graph of linear interpolation of selected work area values of phase II [2]

$$y = -14,929x + 82,547 \quad (9)$$

$$R^2 = 0,971 \quad (10)$$

3.3 Results of experimental phase III

The calculated values of the corrected current (Table 3) of the experimental phase III were shown as the polynomial dependence in the (Figure 8), described by formulas (11), (12).

Table 3 Errors and correct values of the phase III - measurement process [4]

	1.	2.	3.	4.
δ_i [mA]	0,00953	0,00938	0,00927	0,00834
IxKOR [mA]	55,29	53,79	52,69	43,39
	5.	6.	7.	8.
δ_i [mA]	0,00683	0,00609	0,00548	0,00433
IxKOR [mA]	28,29	20,89	14,79	3,29
	9.	10.	11.	12.
δ_i [mA]	0,00415	0,00412	0,00411	0,00411
IxKOR [mA]	1,49	1,19	1,09	1,09
	13.	14.	15.	16.
δ_i [mA]	0,0041	0,00412	0,00415	0,0041
IxKOR [mA]	0,99	1,19	1,49	0,99
	17.	18.	19.	20.
δ_i [mA]	0,0041	0,0041	0,00412	0,00411
IxKOR [mA]	0,99	0,99	1,19	1,09

The shape of the linear waveform is shown in the figure (Figure 9). It can be seen from the graph that the values obtained from the pulse laser at 500 Hz are decreasing faster to zero and differ more from linearity than at a higher frequency.

EXPERIMENTAL VERIFICATION OF OBJECT LEVITATION BY OPTICAL SENSOR

Erik Prada; Ivan Virgala; Martin Varga

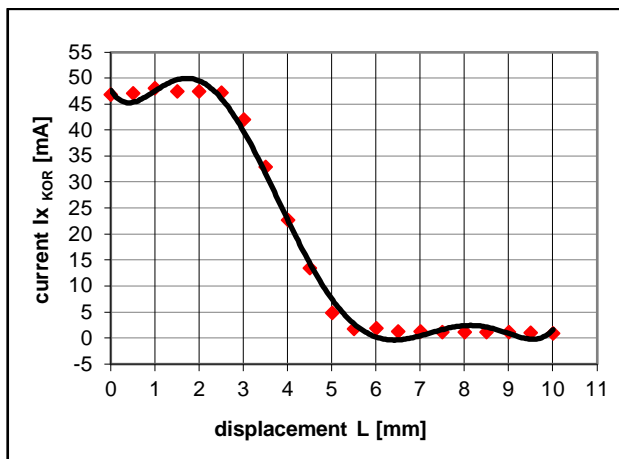


Figure 8 Graph of interpolation of corrected current versus cover length – phase III [2]

$$y = -0,0024x^6 + 0,0918x^5 - 1,3532x^4 + 9,4181x^3 - 28,958x^2 + 17,816x + 54,157 \quad (11)$$

$$R^2 = 0,9949 \quad (12)$$

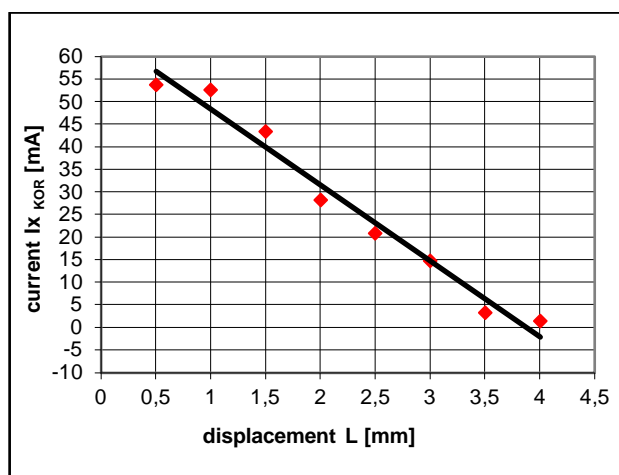


Figure 9 Graph of linear interpolation of selected work area values of phase III [2]

$$y = -16,817x + 65,165 \quad (13)$$

$$R^2 = 0,9747 \quad (14)$$

Conclusions

From the experimental verification of the shadow method for the purpose of determining the position of the levitating object and for the subsequent need for regulation, we found that the dependencies of the corrected values of the individual phases of measurement differ slightly from each other. For the purpose of positioning we are interested mainly in the linear course of the corrected values depending on the displacement of the object [11-12].

Acknowledgement

The authors would like to thank to Slovak Grant Agency – project KEGA 018TUKE-4/2018 “Implementation of new technologies and educational methods in the field of control systems to improve education level and practical skills of graduates of Mechatronics” and project VEGA 1/0389/18, “Research and development of kinematic redundant mechanisms”.

References

- [1] REICH, Š.: *Design of functional model of magnetic levitation*, Diploma thesis, Kosice, TU-SjF, 2003. (Original in Slovak)
- [2] PRADA, E.: *Contactless sensor for positioning of levitating object*, Final thesis, Kosice, TU-SjF, 2009. (Original in Slovak)
- [3] GMITERKO, A., KELEMEN, M., DOVICA, M., CAPÁK, M.: *Miniature mobile robot for moving in a tube with small diameter*, Proceedings of the 2nd International Conference Mechatronics and Robotics '99, Brno, Czech Republic, pp. 67-70, 1999.
- [4] KELEMEN, M., GMITERKO, A., GÓTS, I.: *Mechatronic concept of bristled in-pipe machine*, ATP Plus, Vol. 2001, pp. 48-52, 2001.
- [5] VITKO, A., JURIŠICA, L., BABINEC, A., DUCHOŇ, F., KLÚČIK, M.: *Some Didactic Problems of Teaching Robotics*, Proceedings of the 1st International Conference Robotics in Education 2010, Bratislava, Slovak University of Technology in Bratislava, pp. 27-30, pp. 67-70, 2010.
- [6] HAVLÍK, Š., HRICKO, J., PRADA, E., JEZŇÝ, J.: *Linear motion mechanisms for fine position adjustment of heavy weight platforms*, TUKE, 2020.
- [7] VIRGALA, I., KELEMEN, M., PRADA, E., LIPTÁK, T.: *Positioning of Pneumatic Actuator Using Open-Loop System*, *Applied Mechanics and Materials*, Vol. 816, pp. 160-164, 2015.
- [8] LIPTÁK, T., DUCHOŇ, F., KELEMENOVÁ, T., PUŠKÁR, M., KELEMEN, M., KURYLO, P., PRADA, E.: *Analysis of Uncertainty of Tilt Measurement with Accelerometer*, *Applied Mechanics and Materials*, Vol. 611, pp. 548-556, 2014.
- [9] PRADA, E., BALOČKOVÁ, L., VALÁŠEK, M.: *Elimination of the Collision States of the Effectors of Industrial Robots by Application of Neural Networks*, *Applied Mechanics and Materials*, Vol. 798, pp. 276-281, 2015.
- [10] PRADA, E., VALÁŠEK, M., GMITERKO, A.: *Simulation and Determination of the Influence of the Gait Function on the Change of the Shape of a Snake-Like Robot*, *Applied Mechanics and Materials*, Vol. 789-790, pp. 636-642, 2015.
- [11] SPANIKOVA, G., SPANIK, P., FRIVALDSKY, M., PAVELEK, M., BASSETTO, F., VINDIGNI, V.: *Electric model of liver tissue for investigation of*

EXPERIMENTAL VERIFICATION OF OBJECT LEVITATION BY OPTICAL SENSOR

Erik Prada; Ivan Virgala; Martin Varga

electrosurgical impacts, *Electrical Engineering*,
Vol. 99, pp. 1185-1194, 2017.

- [12] KONIAR, D., HARGAS, L., SIMONOVA, A.,
HRIANKA, M., LONCOVÁ, Z.: *Virtual
Instrumentation for Visual Inspection in Mechatronic
Applications*, 6th Conference on Modelling of
Mechanical and Mechatronic Systems (MMaMS)
Location: High Tatras, SLOVAKIA, pp. 227-234,
2014.

Review process

Single-blind peer review process.

ADAPTABLE MOBILE ROBOT FOR ROUGH TERRAIN

Michal Kelemen; Filip Filakovský; Peter Ferenčík

doi:10.22306/am.v4i4.51

ADAPTABLE MOBILE ROBOT FOR ROUGH TERRAIN
Michal Kelemen

 Technical University of Kosice, Faculty of Mechanical Engineering, Letna 9, Kosice, Slovak Republic, EU,
 michal.kelemen@tuke.sk (corresponding author)

Filip Filakovský

 Technical University of Kosice, Faculty of Mechanical Engineering, Letna 9, Kosice, Slovak Republic, EU,
 filip.filakovsky@tuke.sk

Peter Ferenčík

 Technical University of Kosice, Faculty of Mechanical Engineering, Letna 9, Kosice, Slovak Republic, EU,
 peter.ferencik@tuke.sk

Keywords: mechatronics, education, mobile robot, embedded systems

Abstract: The paper deals with didactic model of mobile four wheeled robot which is able to adapt to rough terrain. The geometry of undercarriage can be changed in accordance with rough terrain. Mechanism for change of chassis clearance is placed in robot body. In case of very rough terrain with large irregularities, the robot can lift own body as prevention of collision with ground. In case when it moves on inclined plane, it can move down own body as prevention before the side overturning.

1 Introduction

Currently, there are many applications, where a mobile robot is better solution for solving of any problems. The application includes also inspection of undercarriage of cars, inspection of mines and caves, fire and rescue tasks, bomb destroying and pyrotechnical tasks, handling the unknown objects, vacuum cleaning, cutting the grass, health care activities, cleaning of floors and walls etc.

The example of the inspection robot (Fig. 1) shows the divided chassis for better crossing through the rough terrain. All wheels are driven with independent motors and controller. This configuration allows to sustain the contact between the wheels and ground. Therefore, the traction of robot is more effective and powerful.



Figure 1 Four wheeled robot with divided chassis

Velocity of rotation is synchronized via using of controller. Direction of locomotion is adjusted with difference of wheel velocity rotation. If obstacle is as stair or street curb, this concept is not useful, because the undercarriage could be locked on irregularities and robot

would not able to locomote. The concept with changeable chassis clearance can solve this problem and in case when irregularities is too high, the clearance is increased to necessary height.

2 Concept of robot undercarriage with changeable chassis clearance

Model of system (Fig. 2) consists of lever mechanism, which is able to adjust clearance of chassis for successful crossing through the irregularities.

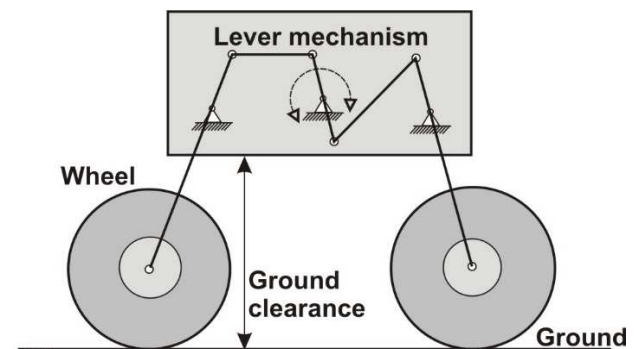


Figure 2 Concept of water tank model

Lever mechanism has been proposed for adjusting of chassis clearance. Left and right side has independent lever mechanism. So, it means that, robot chassis can be adjusted to the different height and it enables to locomote on tilted terrain. It will help to prevent to side overturning.

ADAPTABLE MOBILE ROBOT FOR ROUGH TERRAIN

Michal Kelemen; Filip Filakovský; Peter Ferenčík

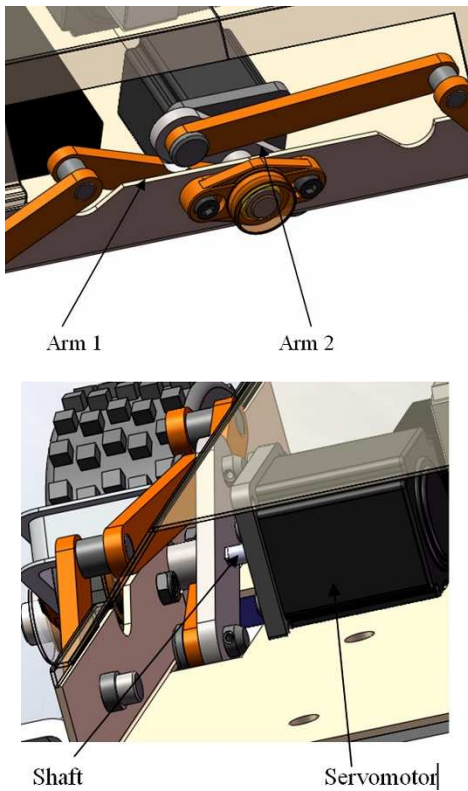


Figure 3 Lever mechanism with servomechanism

The setting of the chassis position is locked with lock mechanism actuated with small servomechanism. There are several default positions where it is possible to lock the adjusted height of chassis. Left and right side has independent lever mechanism and also servomechanism with locking system.

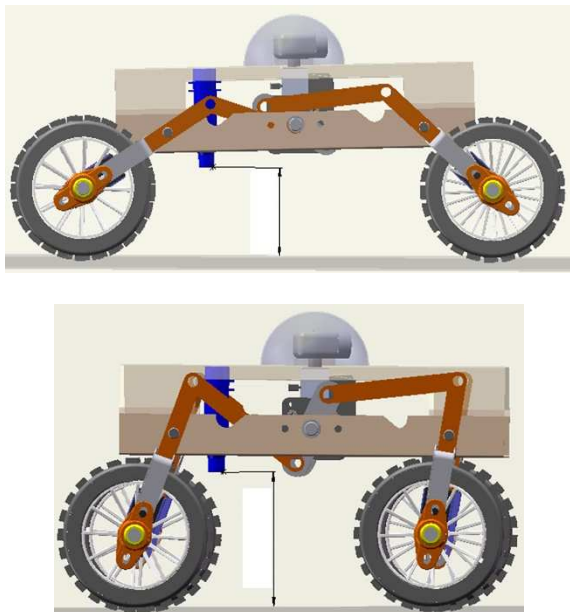


Figure 4 Change of the position of robot chassis

Distance between the chassis and ground is detected via using of optical distance sensors and control system can change automatically chassis clearance.

Lever mechanism consist of two arm levers for synchronized moving with both wheels on chassis. Moving of levers is ensured with servomechanism (Fig. 3).

This concept allows to set the chassis clearance to relatively large range of clearance (Fig. 4)

Selection of suitable servomechanism has been made on the base of static analysis results (Fig. 5) and simulation results (Fig. 6) which shows the all positions from the viewpoint of loading force and torque.

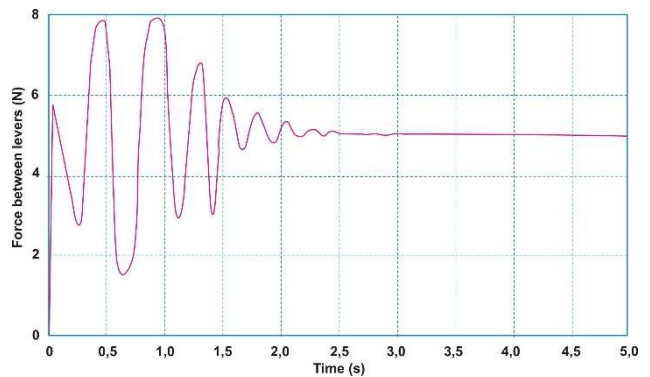


Figure 5 Static analysis of lever

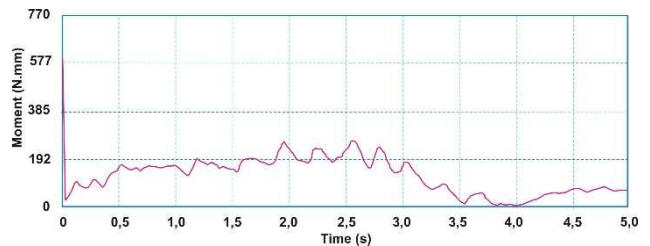


Figure 6 Simulation of lever motion for selection of servomechanism

3 Design of robot parts

Every wheel is driven the separate BLDC motor. Simulation of locomotion has been executed and it shows the requirements on torque on output shaft before wheels (Fig. 7). The extreme value on starting point of the dependence is related to rotation starting and it is typical for this type of motion.

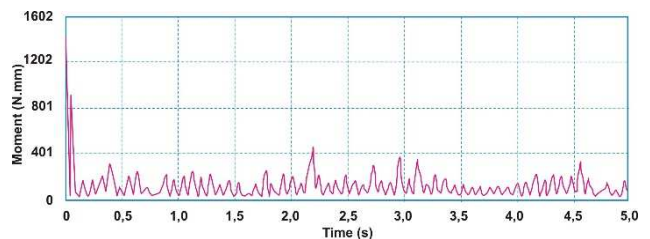


Figure 7 Simulation of locomotion for selection of drive servomechanism for wheels

ADAPTABLE MOBILE ROBOT FOR ROUGH TERRAIN

Michal Kelemen; Filip Filakovský; Peter Ferenčík

Motor is completely placed into wheel for because of space saving and there is no need for system of motion transfer from drive to wheel (Fig. 8 and Fig. 9). This concept brings the contribution of mass saving because the overall weight is significantly decreased. Selected drive motor is supplied also with gearing and control unit with sensors.

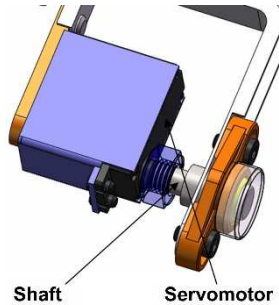


Figure 8 Drive and bearing for output shaft

Special focus has been done to design of bearing system for output shaft (Fig. 8), which will carry the load and vibration coming from the contact between the wheel and ground.

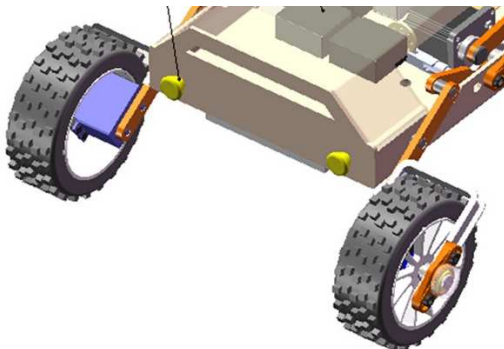


Figure 9 Wheel drive placement inside wheels

Finite element method analysis has been used for checking of the suitable design of chassis part (Fig. 10, Fig. 11, Fig. 12, Fig. 13).

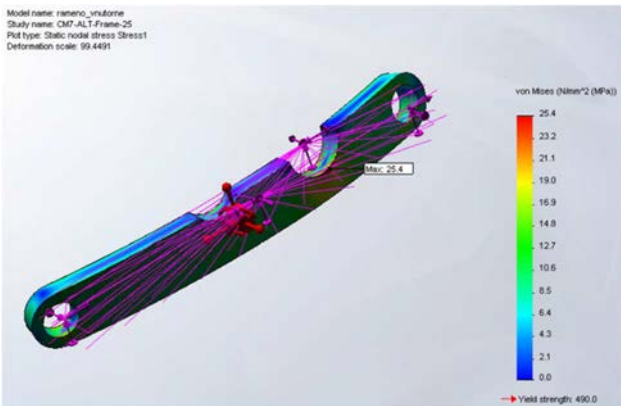


Figure 10 Finite element method analysis – von Misses stresses in lever

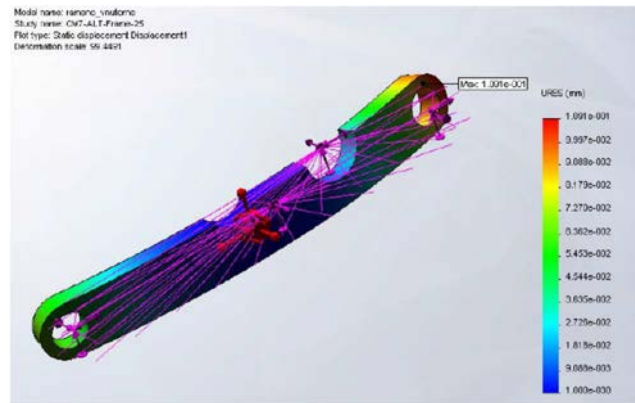


Figure 11 Finite element method analysis – displacements in lever

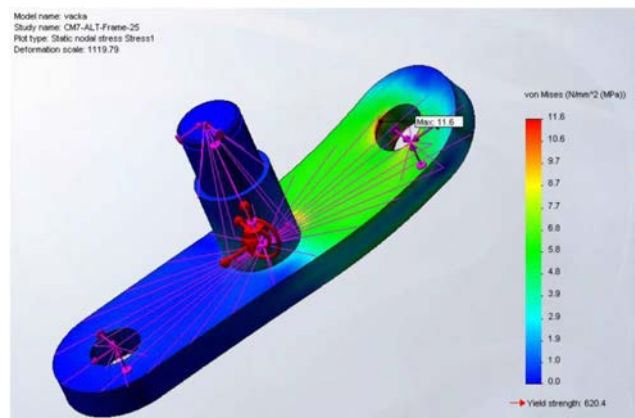


Figure 12 Finite element method analysis – von Misses stresses in cam

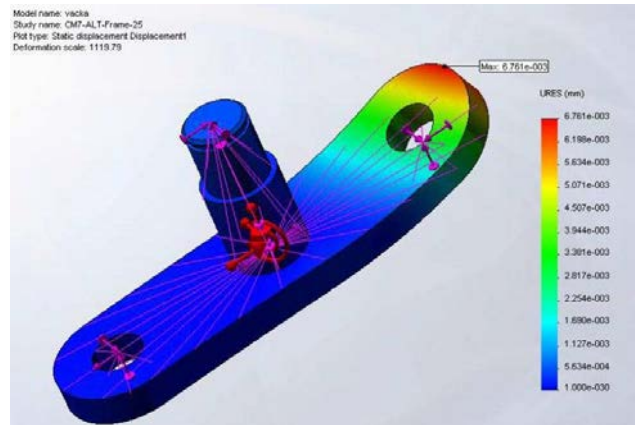


Figure 13 Finite element method analysis – displacements in cam

4 Overall design of the robot

Overall design (Fig. 14) also includes the lights (1) for better visibility of scene before the robot. The locking mechanisms (2) are placed inside the robot body near the lever mechanisms. CCD camera (3) is placed on the top of the robot for visual feedback for teleoperation controlling. Communication unit for wireless teleoperation control (4)

ADAPTABLE MOBILE ROBOT FOR ROUGH TERRAIN

Michal Kelemen; Filip Filakovský; Peter Ferenčík

is also installed on the robot body. Robot is powered by the two batteries placed in back side of the robot body.

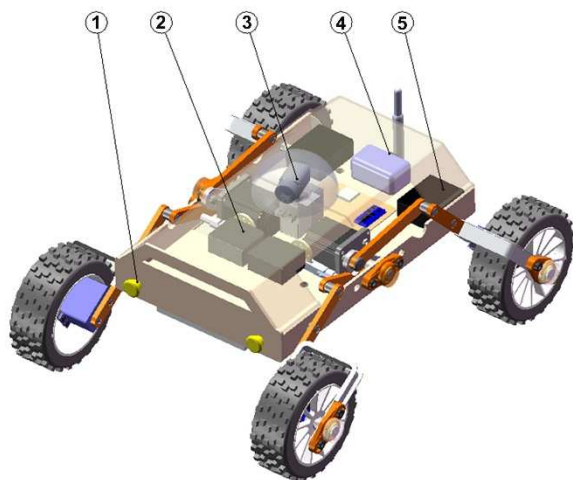


Figure 14 Overall design of the robot

Collision sensors (Fig. 15) are also placed on the robot body and they are used as automatically operated system for collision prevention to avoid of robot damage. The sensors use ultrasonic principle for detection of obstacles.

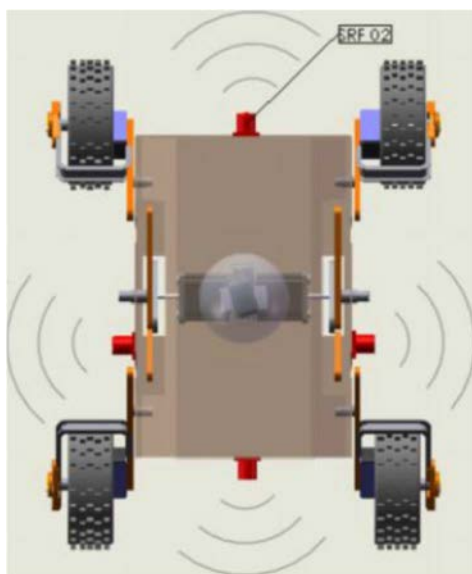


Figure 15 Collision sensors on the robot

5 Conclusion

The aim of this work is to design the mobile robot for locomotion on rough terrain. Irregularities often are bigger than clearance of the robot. It can be solved via using of bigger wheels and higher chassis, but we lost the advantage of low-profile chassis for cases, where we have so much space for robot locomotion. For this reason, it is necessary to adapt chassis clearance in accordance with irregularities height. Also, if robot locomotes on side tilted terrain, the robot can adjust only one side of robot chassis, for sustain

the stability of the robot. Centre of gravity is moved into suitable position for reaching of stable locomotion. This adaptation should be automatically executed. The robot will take care about yourself for safely locomotion. There is also other application, where the intelligent properties of products help to prevent the collisions or other accidents [3-17].

Acknowledgement

The authors would like to thank to Slovak Grant Agency – project VEGA 1/0872/16 supported by the Ministry of education of Slovak Republic.

References

- [1] WANG, B., REN, J., CAI, M.: *Car-Like Mobile Robot Path Planning in Rough Terrain With Danger Sources*, IEEE 2019 Chinese Control Conference (CCC), Date of Conference: 27-30 July 2019, Conference Location: Guangzhou, China, China, Publisher: IEEE, doi:10.23919/ChiCC.2019.8866121.
- [2] HIRAMATSU, T., MORITA, S., PENCELLI, M., NICCOLINI, M., RAGAGLIA, M., ARGJOLAS, A.: *Path-Tracking Controller for Tracked Mobile Robot on Rough Terrain*, *World Academy of Science, Engineering and Technology International Journal of Electrical and Computer Engineering*, Vol. 13, No. 2, pp. 59-64, 2019.
- [3] ZHOU, F., XU, X., XU, H., CHANG, Y., WANG, Q., CHEN, J.: *Implementation of a Reconfigurable Robot to Achieve Multimodal Locomotion Based on Three Rules of Configuration*. *Robotica*, Vol. 2019, pp. 1-17. doi:10.1017/S0263574719001589
- [4] ZHOU, F.-L., XU, X.-J., XU, H.-J., ZHANG, X.: *A Multimodal Hybrid Robot with Transformable Wheels*, *Proceedings of the IEEE International Conference on Real-time Computing and Robotics*, Okinawa, Japan 2017 pp. 139-144, 2017.
- [5] VITKO, A., JURIŠICA, L., BABINEC, A., DUCHOŇ, F., KLÚČIK, M.: *Some Didactic Problems of Teaching Robotics*, *Proceedings of the 1st International Conference Robotics in Education 2010*. Bratislava, 16.-17. 9. 2010, Bratislava, Slovak University of Technology in Bratislava, pp. 27-30, 2010.
- [6] KONIAR, D., HARGAS, L., SIMONOVA, A., HRIANKA, M., LONCOVÁ, Z.: *Virtual Instrumentation for Visual Inspection in Mechatronic Applications*, 6th Conference on Modelling of Mechanical and Mechatronic Systems (MMaMS) Location: High Tatras, SLOVAKIA, pp. 227-234, 2014.
- [7] van BEEK, T. J., ERDENA M. S., TOMIYAMAA, T.: *Modular design of mechatronic systems with function modeling*, *Mechatronics*, Vol. 20, No. 8, pp. 850-863, 2010.
- [8] WANG, Y., YUA, Y., XIEA, Ch., WANGA, H., FENG, X.: *Mechatronics education at CDHAW of Tongji University: Laboratory guidelines, framework,*

ADAPTABLE MOBILE ROBOT FOR ROUGH TERRAIN

Michal Kelemen; Filip Filakovský; Peter Ferenčík

- implementations and improvements, *Mechatronics*, Vol. 19, No. 8, pp. 1346-1352, 2009.
- [9] KELEMEN, M., KELEMENOVÁ, T., JEZNY, J.: Four legged robot with feedback control of legs motion, *Bulletin of Applied Mechanics*, Vol. 4, No. 16, pp. 115-118, 2018.
- [10] DUCHOŇ, F., HUBINSKÝ, P., HANZEL, J., BABINEC, A., TÖLGYESSY, M.: Intelligent Vehicles as the Robotic Applications, *Procedia Engineering*, Vol. 48, pp. 105-114, 2012.
- [11] KONIAR, D., HARGAŠ, L., ŠTOFAN, S.: Segmentation of Motion Regions for Biomechanical Systems, *Procedia Engineering*, Vol. 48, pp. 304-311, 2012.
- [12] BOŽEK, P., CHMELÍKOVÁ, G.: *Virtual Technology Utilization in Teaching*, Conference ICL2011, September 21 -23, 2011 Piešťany, Slovakia, pp. 409-413, 2011.
- [13] TURYGIN, Y., BOŽEK, P.: Mechatronic systems maintenance and repair management system, *Transfer of innovations*, Vol. 26, pp. 3-5, 2013.
- [14] HARGAŠ, L., HRIANKA, M., KONIAR, D., IZÁK, P.: *Quality Assessment SMT Technology by Virtual Instrumentation*, Applied Electronics 2007, Pilsen, 2007.
- [15] SPANIKOVA, G., SPANIK, P., FRIVALDSKY, M., PAVELEK, M., BASSETTO, F., VINDIGNI, V.: Electric model of liver tissue for investigation of electrosurgical impacts, *Electrical Engineering*, Vol. 99, pp. 1185-1194, 2017.
- [16] KARAVAEV, Y. L., KILIN, A. A.: Nonholonomic dynamics and control of a spherical robot with an internal omniwheel platform: Theory and experiments, *Proceedings of the Steklov Institute of Mathematics*, Vol. 295, No. 1, pp. 158-167, 2016.
- [17] KURIC, I., BULEJ, V., SAGA, M., POKORNÝ, P.: Development of simulation software for mobile robot path planning within multilayer map system based on metric and topological maps, *International Journal of Advanced Robotic Systems*, Vol. 14, No. 6, pp. 1-14, 2017.
- [18] KIM, Y.-S., JUNG, G.-P., KIM, H., CHO, K.-J. AND CHU, C.-N.: *Wheel Transformer: A Miniaturized Terrain Adaptive Robot with Passively Transformed Wheels*, Proceedings of the IEEE/RSJ International Conference on Robotics and Automation, Karlsruhe, Germany, pp. 5625-5630, 2013.
- [19] LEE, D.-Y., KOH, J.-S., KIM, J.-S., KIM, S.-W., CHO, K.-J.: Deformable-wheel robot based on soft material, *International Journal of Precision Engineering and Manufacturing*, Vol. 14, No. 8, pp. 1439-1445, 2013.
- [20] MATSUNO, F., TADOKORO, S.: *Rescue Robots and Systems in Japan*, Proceedings of the IEEE International Conference on Robotics and Biomimetics, New Orleans, LA, USA, pp. 12-20, 2004.
- [21] BRUZZONE, L., QUAGLIA, G.: Review article: Locomotion systems for ground mobile robots in unstructured environments, *Mechanical Sciences*, Vol. 3, No. 2, pp. 49-62, 2012.
- [22] VIRGALA, I., MIKOVÁ, E., KELEMEN, M., HRONCOVÁ, D.: Snake-like robots, *Acta Mechatronica*, Vol. 3, No. 4, pp. 7-10, 2018. doi: 10.22306/am.v3i4.43
- [23] MIKOVÁ, E., VIRGALA, I., KELEMEN, M.: Embedded systems, *Acta Mechatronica*, Vol. 3, No. 2, pp. 1-5, 2018. doi:10.22306/am.v3i2.32
- [24] KELEMENOVÁ, T., FRANKOVSKÝ, P., VIRGALA, I., MIKOVÁ, E., KELEMEN, M., DOMINIK, L.: Educational models for mechatronic courses, *Acta Mechatronica*, Vol. 1, No. 4, pp. 1-6, 2016.
- [25] LIPTÁK, T., KELEMEN, M., GMITERKO, A., VIRGALA, I., HRONCOVÁ, D.: THE CONTROL OF HOLONOMIC SYSTEM, *Acta Mechatronica*, Vol. 1, No. 2, pp. 15-20, 2016.
- [26] PIRNÍK, R., HRUBOŠ, M., NEMEC, D., BOŽEK, P.: Navigation of the autonomous ground vehicle utilizing low-cost inertial navigation, *Acta Mechatronica*, Vol. 1, No. 1, pp. 19-23, 2016.

Review process

Single-blind peer review process.

doi:10.22306/am.v4i4.52

AIRFLOW MEASUREMENT TEST DEVICE FOR AIRFLOW SENSORS

Tatiana Kelemenová

Technical University of Kosice, Faculty of Mechanical Engineering, Letna 9, Kosice, Slovak Republic, EU,
tatiana.kelemenova@tuke.sk

Keywords: measurement, education, airflow, anemometer

Abstract: The paper deals with didactic model of test device for testing of airflow sensors and measurement equipment's. The test device contains from source of wind flow with regulator, flow channel with place for the testing of airflow sensors or anemometers. Students can have training with working with sensors and measurements equipment's and also experience with calibration and verification of sensors.

1 Introduction

Nowadays, there are many applications where it is necessary to measure airflow velocity. This measurement is possible to divide into two main groups as:

- Airflow measurements in opened channels.
- Airflow measurements in closed channels.

Area of meteorology uses airflow measurements for weather-forecast. The anemometers are used for the measurement of flow of wind.

Closed channel is represented with tube or pipe and for measurement of airflow is used pitot and Prandtl pipe.



Figure 1 Cup wind anemometer

There are several principles of measurement of airflow. Venturi device is based on principle of reduction of cross-section of flow which causes a pressure differential before and after the cross-section reduction. Airflow measurements is derived from pressure measurement.

Similar principle based on pressure difference uses orifice plate with exactly defined hole diameter and thickness.

Rotameters (Fig. 2) are also famous principle of measurement of airflow. Principle is based on flow of air through the tube with continually increased cross-section where float is lifted with airflow. Float is stabilized in

position where gravity force and force from flow are in equilibrium. This position gives information about the airflow velocity.

Ultrasonic principle is principle, where we cannot change anything inside tube. Ultrasonic transducer is attached to outer side of pipe wall and uses two type of principle as Doppler principle and time to flight principle.

Cup wind anemometer is used for airflow measurement on opened space also frequently called as wind speed anemometer. Change of wind speed causes the change of velocity rotation of vertical shaft with horizontal arms with spherical cups (Fig. 1).



Figure 2 Rotameter

Vane anemometer (Fig. 3) is also suitable for wind speed measurement. It uses the propeller on horizontal axis in wind direction.



Figure 3 Vane anemometer

AIRFLOW MEASUREMENT TEST DEVICE FOR AIRFLOW SENSORS

Tatiana Kelemenová

Hot-wire (Fig. 4) anemometer uses the thin wire, which is electrically heated. Airflow causes the decreasing of wire temperature.



Figure 4 Hot wire anemometer

Controller has to compensate it with higher electric current which gives information about airflow velocity measurement. Advantage is that, there is no moving parts [1-5].

2 Testing device for airflow measurement

Model of system consists of big fan BL6800 as source of airflow with tube for stabilization of airflow and Prandtl tube also called as pitot static tube (Fig. 5) used as reference measurement of airflow.

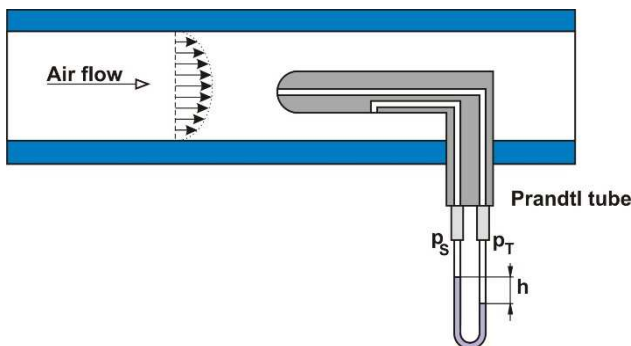


Figure 5 Concept of Prandtl tube measurement

Prandtl tube has one tube hole in flow direction which measures the total pressure composed from static pressure and dynamic pressure. Second input hole – static port is placed on side of Prandtl probe. Both input ports are connected with output terminal on Prandtl tube (Fig. 5). Both terminals are connected to U-tube manometer for measurement of pressure difference. Also, different type of manometer can be used. U-type manometer can be used only in vertical position, because it includes liquid filling.

The velocity of airflow along the cross-section is not constant. The configuration with static pitot tube also allows the measurement of velocity profile of airflow along the cross-section of tube, where we measure airflow velocity. Pitot tube is also used for velocity measurement of aeroplane. In this case pitot tube also includes heater as

prevention of frost cover, which can disable the functionality of pitot tube.



Figure 3 Prandtl tube with input and output ports.

Blower MASTER BL 6800 (Fig. 4) has been used as source of airflow. This is an excellent source because it provides air pressure 388Pa and air displacement 3900m³/h. It has robust and stable design.



Figure 4 Blower MASTER BL 6800

It has terminal with bayonet lock for connecting of tube. Blower has one constant speed and for our purpose it is connected with speed controller RS 10,0 T (Fig. 5). It is normally used in ventilation and air conditioning systems to control the output of single-phase fans by means of smooth variation of the voltage supplied to the motor. The controller operation is based on changing the output voltage. The controller body is made of non-combustible thermoplastic. The controller is equipped with an ON/OFF button. The power output is modulated from 25 to 100%.

AIRFLOW MEASUREMENT TEST DEVICE FOR AIRFLOW SENSORS

Tatiana Kelemenová



Figure 5 Speed controller RS 10,0 T

Overall setting up is shown on figure 6. Blower (1) is connected to the conical reduction (2) and stabilization tube (3). Speed controller (4) is connected to the blower (1). Hot wire anemometers (5) and (6) are tested and installed in hole. Also, vane anemometer (7) is installed for testing.

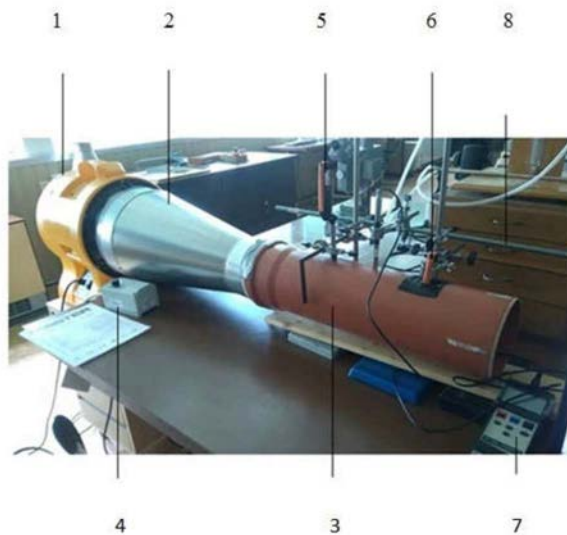


Figure 6 Change of the position of robot chassis

All tested anemometers (Fig. 7) are compared with static pitot tube. Data from all tested anemometers will be compared.

Velocity of airflow measured on pitot tube is defined with equation:

$$w = \sqrt{2 \cdot \frac{p_d}{\rho}} = \sqrt{2 \cdot \frac{q \cdot s}{\rho}} \quad (1)$$

Where

w – airflow velocity; q – kinetic pressure; ρ – air density; p_d – dynamic pressure p_T – total pressure; s – compress ability (liquids $s=1$; gasses $s \neq 1$).

For kinetic pressure it is possible to derive equation:

$$q = \frac{\rho}{2} \cdot w^2 \quad (2)$$

Pressure difference can be measured via using the U-tube and for this case it can be derived as:

$$\Delta p = p_T - p_S = h \cdot \rho \cdot g \quad (3)$$

Where h is height of liquid bar in U-tube and g is gravitational constant.



Figure 6 Vane anemometer and two hot wire anemometers

3 Experimental results

All mentioned anemometers are tested on designed testing device. Ten measurements measured during the constant velocity is shown on figure 7.

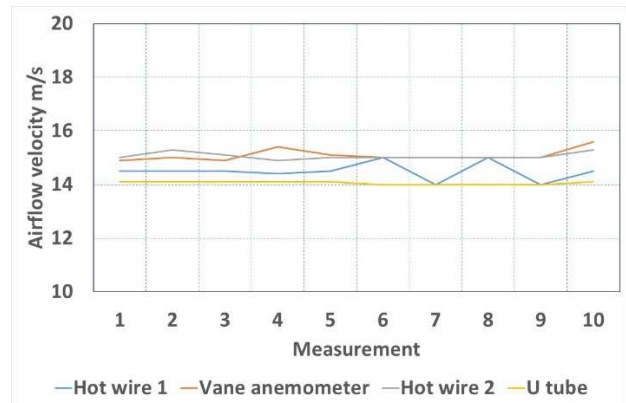


Figure 7 Simulation of locomotion for selection of drive servomechanism for wheels

Measured data are relatively stable and it is close to the reference value. Blower has been adjusted to ten different values and it brought the ten various values of airflow velocity. From this data the averages have been done for comparing the results with reference value. It is shown on figure 8.

AIRFLOW MEASUREMENT TEST DEVICE FOR AIRFLOW SENSORS

Tatiana Kelemenová

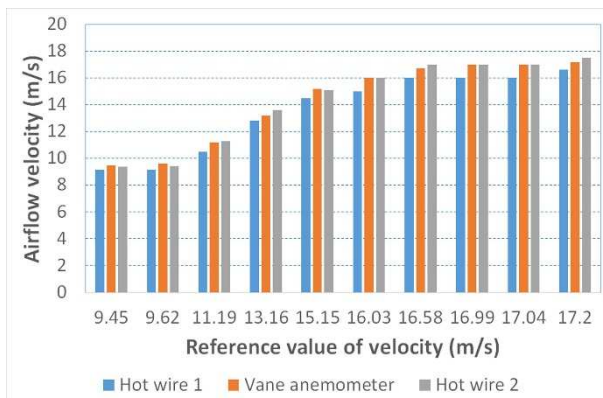


Figure 8 Verification of anemometers value with reference value

After comparing with reference value, measurement error is shown on figure 9. Vane anemometer has the best results from the viewpoint of measurement error.

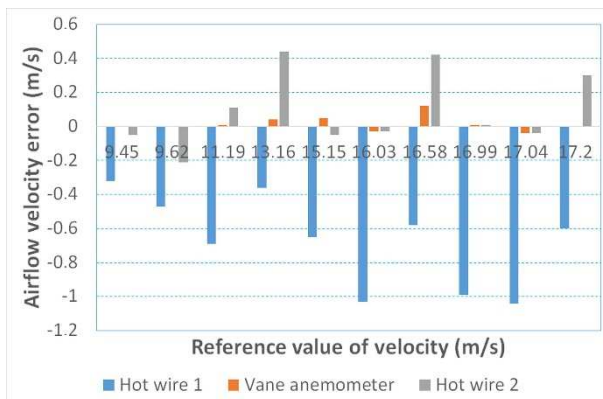


Figure 9 Airflow measurement error

On the base of valid standards [6-9], it is possible to make computation of uncertainty of measurements for comparison of measuring devices (fig. 10).

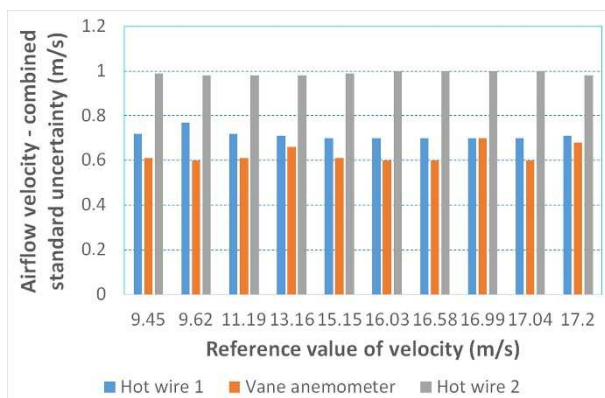


Figure 10 Combined uncertainty of airflow measurements

Vane anemometer also has the best values of combined uncertainty of measurements (fig. 10).

4 Conclusion

The aim of this work was to build the test device and to make a test the available anemometers. The best results have a vane anemometer. On the base of these results, it is possible to declare the uncertainty of measurements and systematic error of measurements.

All measure device should be periodically verified for accessible measurement error and uncertainty fir receive the valid results of measurements [10-26].

Acknowledgement

The work has been accomplished under the research project APVV-15-0149, VEGA 1/0224/18, KEGA 006STU-4/2018 financed by the Slovak Ministry of Education.

References

- [1] KLOPFENSTEIN Jr., R.: Air velocity and flow measurement using a Pitot tube, *ISA Transactions*, Vol. 37, No. 4, pp. 257-263, 1998. doi:10.1016/S0019-0578(98)00036-6
- [2] YANOVYCH, V., DUDA, D., HORÁČEK, V., URUBA, V.: *Research of a wind tunnel parameters by means of cross-section analysis of air flow profiles*. AIP Conference Proceedings 2189, 020024, 2019. doi:10.1063/1.5138636
- [3] TODA, Y., MORIMATSU, M., NISHIO, Y., OGAWA, T.: *Theoretical Model of a Flow in a Tube With a Slit*, ASME-JSME-KSME 2019 8th Joint Fluids Engineering Conference, July 28–August 1, 2019, San Francisco, California, USA. Volume 3A: Fluid Applications and Systems, Paper No: AJKFluids2019-5257, V03AT03A041, pp. 5, 2019. doi:10.1115/AJKFluids2019-5257.
- [4] FRANCO, L. G., RAMOS, R., MATTOS, M. C., ANDRADE, L. A.: *Uncertainty evaluation and experimental analysis fora wind tunnel as reference to gas flare flow measurement*, ENCIT 2018-0041 17th Brazilian Congress of Thermal Sciences and Engineering, November 25th-28th, 2018, Águas de Lindóia, SP, Brazil, 2018.
- [5] EA-4/02 M:2013 *Evaluation of the Uncertainty of Measurement In Calibration*, Publication Reference, European Accreditation Laboratory Committee, September 2013 rev 01. cited August 8th, 2019, Online, Available: <https://european-accreditation.org/wp-content/uploads/2018/10/ea-4-02-m-rev01-september-2013.pdf>
- [6] JCGM 200:2012, *International vocabulary of metrology – Basic and general concepts and associated terms (VIM)*, 3rd edition, BIPM, 2012.
- [7] JCGM 100 – *Evaluation of measurement data – Guide to the expression of uncertainty in measurement (ISO/IEC Guide 98-3)*, 1st edition, September 2008, Online, Available: <http://www.iso.org/sites/JCGM/GU>

AIRFLOW MEASUREMENT TEST DEVICE FOR AIRFLOW SENSORS

Tatiana Kelemenová

- M-JCGM100.htm, http://www.bipm.org/en/publications/guides/gum_print.html
- [8] MSA-L/11 *Guidelines on the expressions of uncertainty in quantitative testing* (EA - 4/16: 2003), Guidelines on the expression of uncertainty in quantitative testing, Slovak national accreditation service, SNAS BRATISLAVA, August 2009. (Original in Slovak)
- [9] MSA-L/12 *Expression of the uncertainty of measurement in calibration*, (EA-4/02) - Expression of the uncertainty of measurement in calibration, Slovak National Accreditation Service, SNAS BRATISLAVA, November 2010. (Original in Slovak)
- [10] PALENCAR, R., SOPKULIAK, P., PALENCAR, J., ĎURIŠ, S., SUROVIK, E., HALAJ, M.: Application of Monte Carlo method for evaluation of uncertainties of ITS-90 by standard platinum resistance thermometer, *Measurement Science Review*, Vol. 17, No. 3, pp. 108-116, 2017.
- [11] WIMMER, G., PALENCAR, R., WITKOVSKÝ, V.: *Stochastic models of measurement*, Graphic studio Ing. Peter Juriga, L. Fullu 13, 841 05 Bratislava, 1st ed., 2001. (Original in Slovak)
- [12] BOŽEK, P., CHMELÍKOVÁ, G.: *Virtual Technology Utilization in Teaching*, Conference ICL2011, September 21-23, 2011 Piešťany, Slovakia, pp. 409-413. 2011.
- [13] TURYGIN, Y., BOŽEK, P.: Mechatronic systems maintenance and repair management system, *Transfer of innovations*, Vol. 26, pp. 3-5, 2013.
- [14] HARGAŠ, L., HRIANKA, M., KONIAR, D., IZÁK, P.: Quality Assessment SMT Technology by Virtual Instrumentation, *Applied Electronics 2007*, 2007.
- [15] SPANIKOVA, G., SPANIK, P., FRIVALDSKY, M., PAVELEK, M., BASSETTO, F., VINDIGNI, V.: Electric model of liver tissue for investigation of electrosurgical impacts, *Electrical Engineering*, Vol. 99, pp. 1185-1194, 2017.
- [16] KARAVAEV, Y. L., KILIN, A. A.: Nonholonomic dynamics and control of a spherical robot with an internal omniwheel platform: Theory and experiments, *Proceedings of the Steklov Institute of Mathematics*, Vol. 295, No. 1, pp. 158-167, 2016.
- [17] KURIC, I., BULEJ, V., SAGA, M., POKORNÝ, P.: Development of simulation software for mobile robot path planning within multilayer map system based on metric and topological maps, *International Journal of Advanced Robotic Systems*, Vol. 14, No. 6, pp. 1-14, 2017.
- [18] KIM, Y.-S., JUNG, G.-P., KIM, H., CHO, K.-J. AND CHU, C.-N.: *Wheel Transformer: A Miniaturized Terrain Adaptive Robot with Passively Transformed Wheels*, Proceedings of the IEEE/RSJ International Conference on Robotics and Automation, Karlsruhe, Germany, pp. 5625-5630, 2013.
- [19] LEE, D.-Y., KOH, J.-S., KIM, J.-S., KIM, S.-W., CHO, K.-J.: Deformable-wheel robot based on soft material, *International Journal of Precision Engineering and Manufacturing*, Vol. 14, No. 8, pp. 1439-1445, 2013.
- [20] MATSUNO, F., TADOKORO, S.: *Rescue Robots and Systems in Japan*, Proceedings of the IEEE International Conference on Robotics and Biomimetics, New Orleans, LA, USA, pp. 12-20, 2004.
- [21] BRUZZONE, L., QUAGLIA, G.: Review article: Locomotion systems for ground mobile robots in unstructured environments, *Mechanical Sciences*, Vol. 3, No. 2, pp. 49-62, 2012.
- [22] VIRGALA, I., MIKOVÁ, E., KELEMEN, M., HRONCOVÁ, D.: Snake-like robots, *Acta Mechatronica*, Vol. 3, No. 4, pp. 7-10, 2018. doi: 10.22306/am.v3i4.43
- [23] MIKOVÁ, E., VIRGALA, I., KELEMEN, M.: Embedded systems, *Acta Mechatronica*, Vol. 3, No. 2, pp. 1-5, 2018. doi:10.22306/am.v3i2.32
- [24] KELEMENOVÁ, T., FRANKOVSKÝ, P., VIRGALA, I., MIKOVÁ, E., KELEMEN, M., DOMINIK, L.: Educational models for mechatronic courses, *Acta Mechatronica*, Vol. 1, No. 4, pp. 1-6, 2016.
- [25] LIPTÁK, T., KELEMEN, M., GMITERKO, A., VIRGALA, I., HRONCOVÁ, D.: THE CONTROL OF HOLONOMIC SYSTEM, *Acta Mechatronica*, Vol. 1, No. 2, pp. 15-20, 2016.
- [26] PIRNÍK, R., HRUBOŠ, M., NEMEC, D., BOŽEK, P.: Navigation of the autonomous ground vehicle utilizing low-cost inertial navigation, *Acta Mechatronica*, Vol. 1, No. 1, pp. 19-23, 2016.

Review process

Single-blind peer review process.

GLUED JOINTS IN THE AUTOMOTIVE INDUSTRY

Silvia Maláková; Anna Guzanová; Peter Frankovský; Vojtech Neumann; Erik Janoško

doi:10.22306/am.v4i4.53

GLUED JOINTS IN THE AUTOMOTIVE INDUSTRY**Silvia Maláková**Technical University of Kosice, Faculty of Mechanical Engineering, Letná 9, Kosice, Slovak Republic,
silvia.malakova@tuke.sk (corresponding author)**Anna Guzanová**Technical University of Kosice, Faculty of Mechanical Engineering, Letná 9, Kosice, Slovak Republic,
anna.guzanova@tuke.sk**Peter Frankovský**Technical University of Kosice, Faculty of Mechanical Engineering, Letná 9, Kosice, Slovak Republic,
peter.frankovsky@tuke.sk**Vojtech Neumann**Technical University of Kosice, Faculty of Mechanical Engineering, Letná 9, Kosice, Slovak Republic,
vojtech.neumann@grob.de**Erik Janoško**Technical University of Kosice, Faculty of Mechanical Engineering, Letná 9, Kosice, Slovak Republic,
erik.janosko@tuke.sk**Keywords:** adhesive, glued joints, finite element method**Abstract:** Glued joints appear in the automotive industry in many types, both in terms of functional stress and in terms of design. Glued joints appear in the automotive industry in many types, both in terms of functional stress and in terms of design. At present, car body plates are most often joined by resistance (spot, seam and projection) welding technology. These disadvantages include, for example, problematic joining of sheets of different thicknesses and qualities, or thermal influencing of the welded area. By using the bonding technology, we avoid these problems and we can take advantage of the many advantages it offers in the automotive industry. This paper gives an overview of the advantages of using glued joints in the automotive industry. It is devoted to the problem of strength calculation of these bonded joints.**1 Introduction**

Many people think that gluing is a modern technique belonging only to the present, but the opposite is true. People have been using adhesives for thousands of years. The first people used glue in the Stone Age. The discovery and introduction of bakelite in 1910 was followed by the introduction of many new types of plastics that are inherently associated with the adhesive. Virtually until World War II, only materials that were able to soak the adhesive (paper, wood) were glued. Glue technology is currently used in construction, aviation or healthcare, and last but not least, in the automotive industry, where adhesives are used not only for bonding body parts, but also for sealing and vibration damping. At present, adhesives are manufactured exactly according to customer requirements and it is difficult to find a field where it would not be used.

Glued joints appear in the automotive industry in many types, both in terms of functional stress and in terms of design. It can be said that the bonding either acts as a complementary and sealing function (bonding and cementing of bodies for sealing, vibration damping, corrosion protection, application of reinforcements) or, in specific cases, can generally represent welding technology in structural strength joints [1-3]. Some applications of glued joints can be seen in Figure 1.

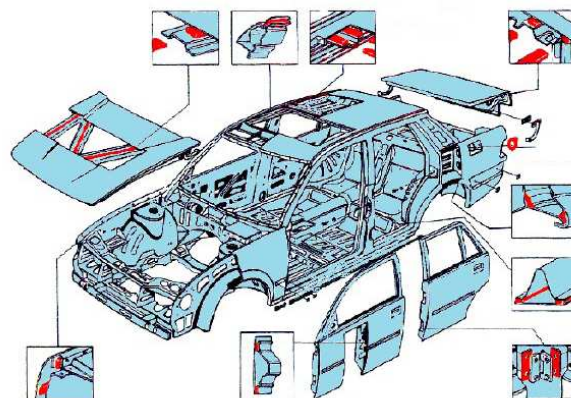


Figure 1 Overview of glued joints of the car body

At present, car body plates are most often joined by resistance (spot, seam and projection) welding technology. This technology has several disadvantages. These disadvantages include, for example, problematic joining of sheets of different thicknesses and qualities, or thermal influencing of the welded area. Other specific problems are caused by the zinc coating, which serves as a corrosion protection in cars. Zinc adheres to the electrodes and there

GLUED JOINTS IN THE AUTOMOTIVE INDUSTRY

Silvia Maláková; Anna Guzanová; Peter Frankovský; Vojtech Neumann; Erik Janoško

is a problem at the weld seams to maintain the protective function of the coating.

By using the bonding technology, we avoid these problems and we can take advantage of the many advantages it offers in the automotive industry. Such as the possibility of new assembly procedures, reduction of the resulting weight of the car, preservation of the protective layer of zinc, higher strength and rigidity of the body, high quality of appearance of the parts to be joined and substantial reduction of noise in the car body.

It also has number of complications with the use of bonding technology in car body construction. For example, the adhesive must be overpainted [4-6], due to production, short time intervals to cure the joint, the adhesive life must be longer than that of a car, the adhesive must have sufficient strength, the shrinkage of the adhesive during curing on the car body surface.

This paper is devoted to the problem of strength calculation of these bonded joints. It deals with classical strength calculation as well as using finite element method for strength calculation.

2 Characteristics of glued joints in the automotive industry

Glued joints appear in the automotive industry in many types, both in terms of functional stress and in terms of design. Adhesives have several obvious advantages over other bonding methods. The main advantages are that they can be used for joining different types and thicknesses of materials without affecting the base material of the parts to be glued compared to other joining technologies such as welding or riveting [7]. Glued joints distribute more evenly under stress, absorb vibration and often perform a sealing function. In spite of all advantages, the strength and load-bearing capacity of the bonded joint depends mainly on its suitable positioning.

The main advantage of joining parts by gluing is the use of this technology where it is not possible to create a joint in other ways e.g. different types of materials, complex shapes, etc. Bonding has many advantages and disadvantages, but this work focuses primarily on the advantages and disadvantages of using adhesive technology in the automotive industry and with regard to the design and stress of the bonded joint.

Advantages of glued joints:

- increased stiffness of the parts to be joined,
- tightness of joints (no need for additional sealing),
- good damping properties (noise, vibration),
- increased safety in case of failure (Figure 2),
- weight loss,
- possibility of joining materials of different sizes and thicknesses,
- increase of corrosion resistance of the car body, both chemical and electrolytic (adhesive is an electrical insulator),

- possibility of joining various materials (steel-glass, rubber-steel etc.),
- no damage to the protective layer of galvanized sheets,
- flat mounting of car body plates ensures uniformly distributed tension in the glued joint (which increases overall strength and rigidity of the whole car body).

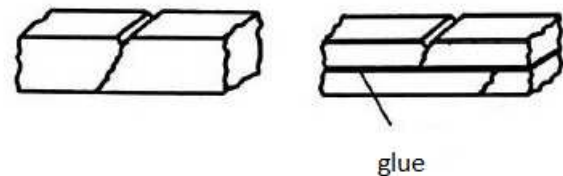


Figure 2 Mitigation of notch effects by adhesive layer [8]

Disadvantages of glued joints:

- technological complexity of preparation of glued surfaces,
- long curing time of the adhesive, maximum strength of the glued joint reaches after some time,
- low temperature resistance,
- aging of the adhesive,
- low peel and splitting strength,
- non-demountability of glued joints.

The nature and composition of the adhesives used to build the car body is always firmly linked to the desired function of the joint. In this way, the adhesives can be divided into strength, reinforcement and sealing [9].

Strength adhesives cure together with body paint. The edge adhesives are partially cured by induction heating during assembly, but full hardness is achieved only during the curing of the varnish by high temperatures in the furnace. The designer currently has a choice of many types of adhesives with different mechanical properties, ranging from tensile to brittle behaviour. In the automotive industry, we are particularly interested in strength adhesives.

3 Calculation of glued joints of glued joints

Glued joints can be loaded statically or dynamically and their material properties are determined primarily for three characteristic load cases: tension, shear and peel. As a rule, the pressure is not specified because the compressive strength of the glued joint is incomparably higher than for other types of stress and is difficult to achieve. These characteristic load cases usually occur in different combinations (e.g. tension - shear, peel - tension). In special cases, however, these load cases can be encountered separately (Figure 3) (e.g. net tension or clean shear).

The glued joints have a high shear resistance. Very badly tolerated tensile force. Therefore, we shape them so that the joint is loaded only by shearing.

GLUED JOINTS IN THE AUTOMOTIVE INDUSTRY

Silvia Maláková; Anna Guzanová; Peter Frankovský; Vojtech Neumann; Erik Janoško

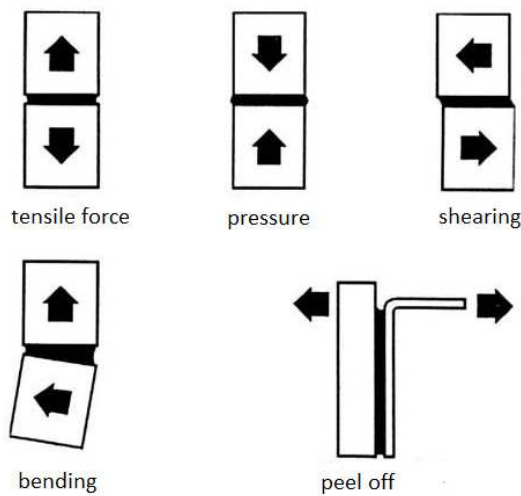


Figure 3 Types of stresses of glued joints

The glued joint is loaded with force F (Figure 4). In this case (assuming the flange material is inelastic), both parts are shifted by length e . If Hook's law applies to the adhesive, the voltage τ is the same over the entire length of the connection l .

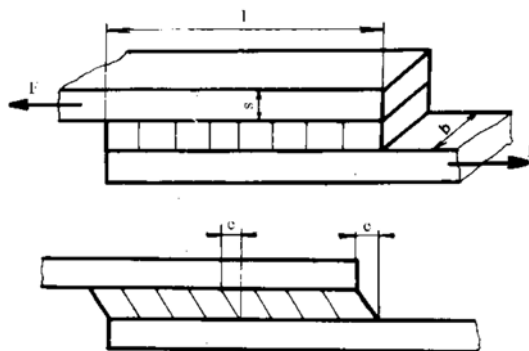


Figure 4 Glued joint stressed on shear

The basic calculation equation (1), (2) is based on the mean stress τ equally distributed over the length of the joint and we compare it with the allowable stress τ_D .

$$\tau = \frac{F}{b \cdot l} \leq \tau_D \quad (1)$$

$$\tau_D = \frac{\tau_p}{k} \quad (2)$$

where k - safety factor, F - force, l - length of the connection, b - joint width, τ - tensile stress, τ_D - allowable tensile stress.

Experiments showed these values (3) τ_p for steel are

$$\tau_p = (23 \div 54) \cdot 10^6 Pa \quad (3)$$

4 Calculation of glued joints using finite element method

Recently, at ever faster evolving computer technology and available literature, we can encounter modern numerical methods, such as finite element method (FEM) [10,11]. It is one of the most widespread numerical mathematical methods used to solve the problems of elasticity and strength, the dynamics of pliable bodies, heat transfer, fluid flow, electromagnetism, and many other problems in engineering.

Knowledge of the behavior of glued joints is essential for their subsequent application in practice. For effective prediction of the properties of glued joints it is necessary to use suitable tools allowing to accurately model various modes of failure that may occur in the structure. The failure of glued joints includes the area from the beginning of loading to the initiation of the crack, followed by the area of development of the failure.

The possibility of numerical simulation of the glued joint is the main requirement for its successful design. If a suitable numerical method was found, it would be possible to replace a large part of the glued joint experiments with this simulation. This would lead to a reduction in the times involved in the development, production and production cost of the product.

The simpler tools offered by FEM analysis allow you to model only the area from the beginning of the load to the initiation of damage [12]. The principles of linear elastic fracture mechanics apply in this area. The behavior in this area is described by the cohesive stiffness of the adhesive layer. The failure initiation state occurs at a critical value of the stress at the crack front. In the FEM model, this state describes the tension between the nodes of an idealized adhesive layer caused by their critical displacement and critical load.

In addition to the strength approach, advanced analyzes can also be based on the elasto-plastic fracture mechanics approach to describe the area of failure development. These principles apply especially in a situation where the adhesive layer is very thin between two parts to be glued and its behavior cannot be described by macroscopic properties, such as tensile modulus or Poisson's constant (E, ν) [13]. In these cases, the behavior of the bonded joint by the energy required for crack propagation, or the rate of release of the strain energy G , is described.

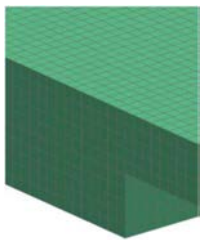
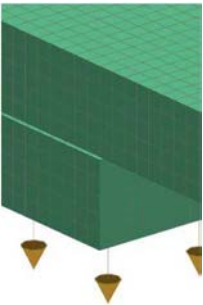
These approaches make it possible to predict the onset and spread of failure without prior knowledge of the location of the crack and the direction of crack propagation in the structure. The quality of the calculation and the accuracy of the results are directly dependent on how ideally the adhesive layer can be idealized using conventional and advanced tools offered by FEM analysis. In addition to the accuracy of the results, the duration of the calculation, these can also differ in the user-friendliness of the results.

GLUED JOINTS IN THE AUTOMOTIVE INDUSTRY

Silvia Maláková; Anna Guzanová; Peter Frankovský; Vojtech Neumann; Erik Janoško

Elements commonly available in FEM analyzes can be used to idealize the adhesive layer. Their behavior is described in terms of material parameters, which in some cases can be obtained from glue producers, but more often it is necessary to find out more difficult by means of experiments. Specifically, the adhesive layer can be replaced by contact, 3D elements, 2D elements, a linear spring system, or simply replacing the adhesive, such as the SSG element in Siemens NX or the TIE element in Abaqus. Individual modeling techniques using 3D elements for adherend realization are shown in Tab. 1. By means of these elements it is possible to describe only the linear area of cohesive behavior of the adhesive, up to the initiation of failure.

Table 1 Comparison of basic modeling techniques [14]

FEM model	The way of idealization Adherend - adhesive layer
	3D - 3D
	3D - 1D Elements with defined stiffness
	3D - Special glued contact

The first step is to create a CAD model. This model is then converted into a preprocessor, which converts the geometric model into the form necessary for the calculation itself. In this phase, the main task is to create an adequate computer network and to define the initial conditions correctly. The preparation of the whole calculation model follows the rules that each company creates itself and must be strictly observed. The rules are set to achieve a

compromise between computational complexity and result accuracy.

The next step is to load the file into the solver and start the calculation itself. The calculation is started using the command line and follows the mathematical operations described above. The results are written to files during the calculation.

The last step is to load and process the results in the postprocessor. The postprocessor allows viewing the simulated process, plotting acceleration, stress, strain and many other variables depending on the selected variable.

In recent years, models using the so-called cohesive joint model have been used in the research of glued joints. The cohesive Model can be used to model adhesives, bonded surfaces, seal models, patches, or delamination processes (Fig.5). The cohesive model exploits some of the advantages of common FEM elements and is based on Griffith's refraction theory. The aforementioned common elements included in the FEM creation tools are characterized by the absence of a criterion for predicting the evolution of violations for any violation mode. The cohesive model is innovative and used approach for the calculation and prediction of the evolution of bonding failure, specifically this model includes, compared to the previously mentioned models, the area of crack initiation in the structure.

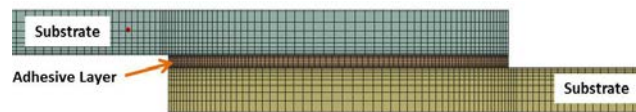


Figure 5 2D plain strain finite element model of bonded joint testing

The cohesive model must be implemented in the numerical model of FEM analysis. All elements making it possible to apply the principles of the cohesive model are generally referred to in the literature as decohesive elements [15]. These elements can be one-dimensional, two-dimensional, and three-dimensional elements and include commonly available solver for FEM analysis. Cohesive elements are used for modeling an adhesive layer with a certain final thickness compared to a cohesive surface contact. The adhesive behavior of these elements is defined by the material properties. Cohesive elements are defined by the thickness, stiffness and strength of the adhesive. It is advisable to apply cohesive elements especially in places where crack development can be expected. It is assumed that at the beginning of loading there are no cracks in the adhesive layer, otherwise this phenomenon can be modeled by the absence of elements at the crack site. The relative displacements between the upper and lower surfaces, which are measured in the thickness direction and in the directions perpendicular, represent the opening of the crack face between the glued surfaces.

GLUED JOINTS IN THE AUTOMOTIVE INDUSTRY

Silvia Maláková; Anna Guzanová; Peter Frankovský; Vojtech Neumann; Erik Janoško

5 Conclusions

Glued joints appear in the automotive industry in many types, both in terms of functional stress and in terms of design. It can be said that the bonding is either complementary and sealing (bonding and cementing of bodies for sealing, vibration damping, corrosion protection, application of reinforcements) or can, in specific cases, represent welding technology in structural strength joints.

The nature and composition of the adhesives used to build the car body is always firmly linked to the desired function of the joint. In this way, adhesives can be divided into strength, reinforcement and sealing, depending on their purpose. Strength adhesives cure together with body car paint. The edge adhesives are partially cured by induction heating during assembly, but full hardness is achieved only during the curing of the varnish by high temperatures in the furnace.

With the development of the automotive industry, the ever-increasing number of cars on the road and the related increase in road accidents, manufacturers are increasingly concerned with the passive safety of cars. When the new vehicle is put into operation, there is a so-called homologation where the car must meet all the requirements specified in the standard. One of the many conditions is that the car must guarantee a prescribed level of passive safety, which is tested under predetermined conditions. At present, we are still looking for possibilities and technologies that would mean cheaper, faster and more accurate production of cars, while maintaining the conditions and criteria required by us. These technologies undoubtedly include computer design of cars. Everything is done on computers from designing, designing individual components, to demanding strength calculations and simulating vehicle barrier tests. In all calculations and simulations, the aim is to bring the computational model to reality as much as possible. Numerical simulation of the glued joint allows to reduce the time for product development, production and production costs.

Acknowledgement

This work is a part of these projects VEGA 1/0154/19 "Research of the combined technologies of joining dissimilar materials for automotive industry", VEGA 1/0290/18 "Development of new methods of determination of strain and stress fields in mechanical system elements by optical methods of experimental mechanics" and APVV-16-0259 "Research and development of combustion technology based on controlled homogenous charge compression ignition in order to reduce nitrogen oxide emissions of motor vehicles".

References

- [1] ŠMIDRIAKOVÁ, M., SEDLIAČIK, J.: Príprava tvrdiva pre melamínformaldehdyové lepidlo na zvýšenie vodovzdornosti lepeného spoja, *Acta facultatis xylologiae Zvolen*, Vol. 52, No. 2, pp. 73-79, 2010. (Original in Slovak)
- [2] DUKARSKA, D., LECKA, J.: Polyurethane foam scrap as MUPF and PF filler in the manufacture of exterior plywood, *Annals of Warsaw University of Life Sciences - SGGW, Forestry and Wood Technology*, Warszawa, Vol. 65, pp. 14-19, 2008.
- [3] KOTTNER, R., KROUPA, T., LAŠ, V., BLAHOŠ, K.: Výpočtový model pro posouzení pevnosti ovýjeného kolíkového spoje kompozit/kov, *Bulletin of Applied Mechanics*, Vol. 2008, pp. 1-6, 2008. (Original in Czech)
- [4] LEE, S. W., LEE, D.: Static and Dynamic Torque Characteristic of Composite Cured Single Lap Joint, *Journal of Composite Materials*, Vol. 31, No. 21, pp. 2188-2201, 1997.
- [5] WALAME, M. V., AHUJA, B. B.: Profile modification of adhesively bonded cylindrical joint for maximum torque transmission capability, *International Journal of Modern Engineering Research*, Vol. 4, No. 8, pp. 1-11, 2013.
- [6] ZEMČÍK, R., LAŠ, V.: Numerical and experimental analyses of the delamination of crossply laminates, *Materiali in Tehnologije*, Vol. 42, No. 4, pp. 171-174, 2008.
- [7] HASSANIEH, A., VALIPOUR, H. R., BRADFORD, M. A., JOCKWER, R.: Glued-in-rod timber joints: analytical model and finite element simulation, *Materials and Structures*, Vol. 51, No. 61, pp. 1-16, 2018.
- [8] HISEM, P.; ELISOVÁ, L.: Využití lepení ve stavbě automobilových karoserií, *Tématický magazín, Svařování - dělení - spojování materiálů*, TM vydavatelství. Praha, pp. 32, 2003. (Original in Czech)
- [9] PETRUŠKA, J.: *Počítačové metody mechaniky II*, Brno, VUT Brno, pp. 96, 2000. (Original in Czech)
- [10] KELEMEN, M., VIRGALA, I., FRANKOVSKÝ, P., KELEMENOVÁ, T., MIKOVÁ, T.: Amplifying system for actuator displacement, *International Journal of Applied Engineering Research*, Vol. 11, No. 15, pp. 8402-8407, 2016.
- [11] CZECH, P., WOJNAR, G., WARCZEK, J.: Diagnostowanie uszkodzeń wtryskiwaczy w silnikach spalinowych pojazdów przy użyciu analizy bispektrum i radialnych sieci neuronowych, *Logistyka*, Vol. 2013, No. 3, pp. 1181-1187, 2013.
- [12] KAŠŠAY, P.: Comparison of pneumatic flexible shaft coupling static load characteristics obtained experimentally and by calculation, *Scientific Journal of Silesian University of Technology, Series Transport*, Vol. 85, No. 1925, pp. 57-65, 2014.
- [13] URBANSKÝ, M.: Theoretic and Experimental Determination of the Flow Resistance Coefficient at

GLUED JOINTS IN THE AUTOMOTIVE INDUSTRY

Silvia Maláková; Anna Guzanová; Peter Frankovský; Vojtech Neumann; Erik Janoško

- Gaseous Medium Flow into and out of the Pneumatic Coupling, *Scientific Journal of Silesian University of Technology*, Vol. 85, No. 1925, pp. 119-125, 2014.
- [14] LAŠOVÁ, V., VACÍK, M., KOSNAR, P., JANDA, R., KOTTNER, DVOŘÁK, J.: *Výzkum spojení kompozitních a kovových částí strojů - Dílčí zpráva V002*, Plzeň, 2011. (Original in Czech)
- [15] CAMANHO, P. P., DAVILA, C. G.: *Mixed-Mode Decohesion Finite Elements for the Simulation of Delamination in Composite Materials*, NASA/TM-2002-211737, 2002.

Review process

Single-blind peer review process.

EVALUATION OF RESIDUAL STRESSES USING OPTICAL METHODS

Ján Kostka; Peter Frankovský; Peter Čarák; Vojtech Neumann

doi:10.22306/am.v4i4.55

EVALUATION OF RESIDUAL STRESSES USING OPTICAL METHODS**Ján Kostka**

Technical University of Kosice, Faculty of Mechanical Engineering, Letna 9, Kosice, Slovak Republic,
jan.kostka@tuke.sk (corresponding author)

Peter Frankovský

Technical University of Kosice, Faculty of Mechanical Engineering, Letna 9, Kosice, Slovak Republic,
peter.frankovsky@tuke.sk

Peter Čarák

Technical University of Kosice, Faculty of Mechanical Engineering, Letna 9, Kosice, Slovak Republic,
peter.carak@tuke.sk

Vojtech Neumann

Technical University of Kosice, Faculty of Mechanical Engineering, Letna 9, Kosice, Slovak Republic,
vojtech.neumann@grob.de

Keywords: optical methods, LF/Z-2, residual stresses, hole drilling

Abstract: The paper deal with quantification of residual stresses by the drilling method and design of the methodology of using optical device LF/Z-2 for their verification. The optical methods have been used for strain analysis for years, but with the continuous development of new and more accurate measuring instruments and devices, are solved the possibilities of creating new application methodologies. For using the Optical PhotoStress method for quantifying residual stresses, has been designed an accurate positioning device to analyse the released deformations around the drilled hole in multiple steps as considering by ASTM E837-13a for drilling methods.

1 Introduction

Determination of causes and the prediction of the failure of the bearing members of structures is still a highly topical issue related to the assessment of the lifetime of structures, machines, equipment, etc. It should be pointed out that many failures of parts of structures, systems or machines are not only due to the stress induced by the load, but are also due to the occurrence of residual stresses. These also occur in unloaded structures or machine parts. They can be caused not only by the operating load, but also by the production technology (casting, rolling, pressing, etc.) as well as by welding. Determining the occurrence of residual stresses, their size and direction is problematic without carrying out experimental measurements. The risk of their occurrence is mainly related to the fact that they are superimposed on operating stresses, which can significantly affect the life of machines and equipment.

For this reason, it is necessary to know and quantify these stresses to predict the occurrence of disorders. Currently, the drilling method is most commonly used to determine residual stresses in the material. This is a semi-destructive experimental method of quantifying residual stresses in a selected point. The authors use the SINT MTS 3000 drilling equipment or the RS 200 drilling machine to solve specific practical tasks.

2 Analysis of the causes of defects in constructions with a combination of hole drilling methods and photoelasticimetry

Despite the advances made in numerical methods, it is still not possible to unambiguously analyse the residual stresses using numerical methods. Therefore, even nowadays experimental methods in the area of detection and measurement of residual stresses have their irreplaceable place. It is necessary to know the individual stages of the experiment when stressing machine components or assemblies with drilling and optical methods and then determining stress and deformation sizes. The aim of this experimental part was to propose a methodology for determining residual stresses using optical methods, namely the PhotoStress method together with hole drilling method [1-12].

American norm ASTM E837-13a is currently the only generally accepted standard that deals with investigating residual stresses by experimental mechanics. However, there are a number of limitations in this standard. For direct drilling into the component and subsequent examination of the deformation values by optical methods, it was necessary to design and manufacture the device (Fig. 1 a, b), which would connect the two mentioned methods of detecting stresses and deformations in structural members. The idea was to design a device with an adjustable drilling head and an optical device for detecting deformation fields - the LF/Z-2 polariscope. The principle was to accurately drill into a defined depth of the component with a special cutting tool. Subsequently, by

EVALUATION OF RESIDUAL STRESSES USING OPTICAL METHODS

Ján Kostka; Peter Frankovský; Peter Čarák; Vojtech Neumann

polariscop, directions and differences of the main proportional deformations were observed. After each step were created images of isoclinic and isochromatic lines (Fig. 5).

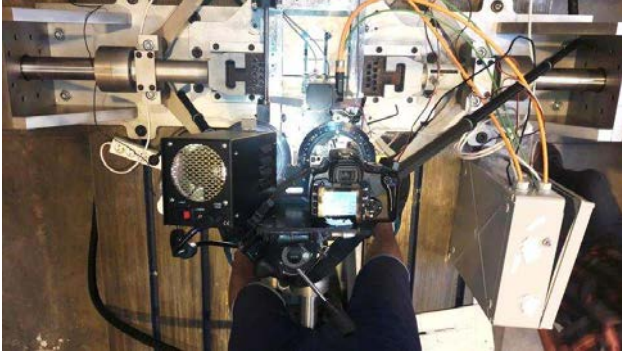


Figure 5 Process of registration of isoclinic and isochromatic lines with a polariscop LF/Z-2

The entire measurement phase without the application of strain gauge and photoelastic coating took approximately 2 hours. At the Fig. 6 is a more detailed time

record of the vertical displacement of the drilling head into the annealed sample registered by the displacement sensor.

In the next section, isochromatic lines for a given depth of 0.5 mm (Fig. 7), 1.0 mm (Fig. 8), 1.5 mm (Fig. 9) and 2 mm (Fig. 10) are given for comparison of the released strain ratios. Blind hole drilling was not realized for larger depths (in accordance with ASTM E 837-13a). From Fig. 7 - Fig. 10 it stands to reason that more pronounced bands (isochromatic lines) are more visible when drilling an annular groove, which corresponds to the results of numerical modeling. Despite this, it can be stated that these are relatively low stress levels, their quantification is more demanding and the measurement inaccuracy is also higher in this case. On the other hand, low levels of simulated "residual" stresses do not pose a risk to the safe operation of machinery and equipment. Higher sensitivity of the simulated stress measurement is possible by using an optically sensitive coating with a greater thickness, which however limits the use of cutting tools (milling cutter or hollow cutter).

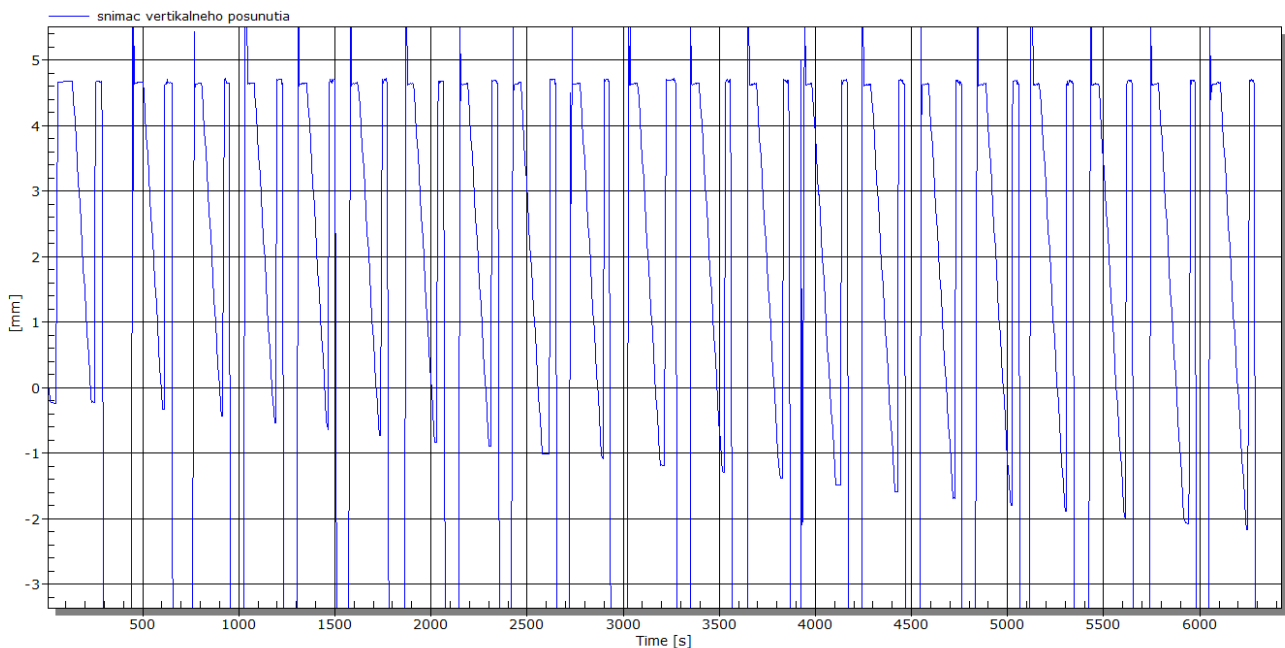


Figure 6 Time recording from vertical movement of hole drilling

Within the proposed methodology of quantification of residual stresses using the PhotoStress method, it was due to the comparison of achieved results with the method of drilling, resp. Ring-Core method considered using identical cutting tools 3.2 mm diameter cutter used with RS-200 and hollow cutter used with SINT-MTS 3000

Ring-Core. The limiting factor is the shape of the cutting tools for drilling the blind hole, respectively. an annular groove, since the thickness of the adhesive and the coating used had to be added to the depth itself. Therefore was used the thinnest coating of PS-1D with a thickness of 0.5 mm.

EVALUATION OF RESIDUAL STRESSES USING OPTICAL METHODS

Ján Kostka; Peter Frankovský; Peter Čarák; Vojtech Neumann

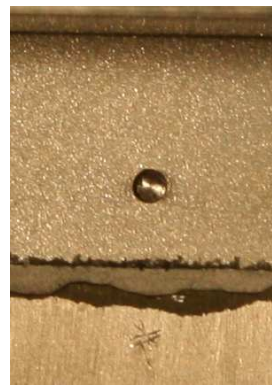


a)



b)

Figure 7 Isochromatic lines for 0.5 mm depth a) blind hole, b) annular groove

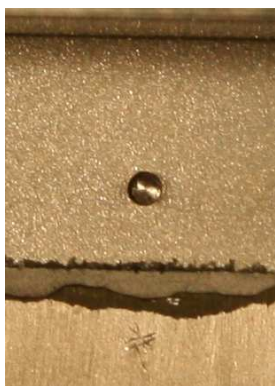


a)



b)

Figure 9 Isochromatic lines for 1.5 mm depth a) blind hole, b) annular groove



a)



b)

Figure 8 Isochromatic lines for 1.0 mm depth a) blind hole, b) annular groove



a)



b)

Figure 10 Isochromatic lines for 2.0 mm depth a) blind hole, b) annular groove

The time recording of the relative deformations in the test sample during the experimental measurements is shown in Fig. 11. It is clear from the figure that there were no significant variations during the measurement, the correct operation has been confirmed of the simulated load-

causing hydraulic load device. The hydraulic loading device can be considered as one of the key elements of the measurement chain, since if the stress in the sample analysed is changed in the experiment, the obtained results could not be considered as relevant.

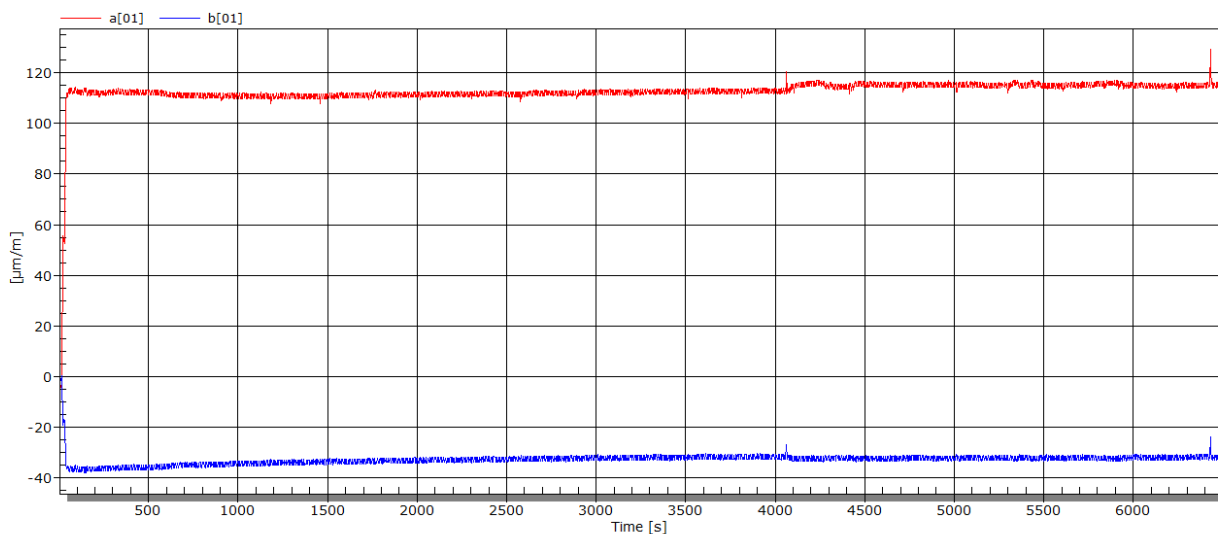


Figure 11 Time recording of relative deformations on loaded test sample

EVALUATION OF RESIDUAL STRESSES USING OPTICAL METHODS

Ján Kostka; Peter Frankovský; Peter Čarák; Vojtech Neumann

Conclusion

In the submitted paper, the methodology of quantification of residual stresses was proposed and verified. On the basis of the results obtained, it can be stated that an accurate positioning device has been designed to evaluate the released relative deformations during the progressive drilling of the blind hole, respectively an annular groove using the PhotoStress optical method. These devices were used in experimental measurements on unloaded samples as well as annealed samples loaded with simulated loads. On the basis of the analysis of isochromatic bands around a 3.2 mm diameter blind hole and around a groove with an outer diameter of 18 mm and an internal diameter of 14 mm registered with a reflection polariscope, it can be concluded that the more visible deformations are around the annular groove. For experimental measurement, the PS-ID coating was chosen to achieve the lower adhesive and coating thickness. The disadvantage of said coating is less sensitivity to the deformation released. It is true that the thicker the coating, the more accurate the measurement. This fact will be dealt with in the next period, as the cutting tools used by RS-200 or SINT-MTS 3000 Ring-Core devices were used in the present work.

The advantage of applying the optical method for quantifying residual stresses is, among other things, the possibility of full-field deformation analysis in the investigated area on a real structure or device. Despite the good consensus of the results obtained by experimental measurement and numerical computation, which is part of the work [17-21], the results achieved cannot be considered final.

There is wide scope for:

- research into the possibility of using the proposed methodology for inhomogeneous, anisotropic, composite materials,
- optimizing the design of the pointing device not only to reduce its weight but also to position it in the third axis, allowing the device to be used for the drilling method, respectively Ring-Core,
- use of the proposed equipment not only for the PhotoStress method, but also in combination with the DIC (Digital Image Correlation) method, with which we also have extensive experience in the area of deformation and stress analysis in the vicinity of concentrators at the KAMASI workplace,
- automating the drilling and strip reading process by compensator, not only significantly reducing the length of the experimental measurement, but also eliminating the adverse effect of the human factor e.g. when positioning the device, etc,
- testing new cutting tools.

Acknowledgements

The authors would like to thank for financial support for this study the Slovak Grant Agency VEGA under grant VEGA no. 1/0290/18.

References

- [1] KOBAYASHI, A. S.: *Handbook on Experimental Mechanics*, Society for Experimental Mechanics, Seattle, 1993.
- [2] PhotoStress® Coatings. Micro-Measurements, [Online], Available: <http://www.vishaypg.com/docs/11222/pscoat.pdf> [12.07.2019], 2019.
- [3] PÁSTOR, M., TREBUŇA, F.: Application of transmission photoelasticity for stress concentration analyses in construction supporting parts, *Applied Mechanics and Materials*, Vol. 611, pp. 443-449, 2014.
- [4] TREBUŇA, F., ŠIMČÁK, F.: *Príručka experimentálnej mechaniky*, TypoPress, Košice, 2007. (Original in Czech)
- [5] TREBUŇA, F., ŠIMČÁK, F., BOCKO, J., TREBUŇA, P.: Failure analysis of mechanical elements in steelworks equipment by methods of experimental mechanics, *Engineering Failure Analysis* 17, pp. 787-801, 2010.
- [6] TREBUŇA, P., TREBUŇA, F., ŠIMČÁK, F.: Analysis of possible causes of cracks initiation on barking drum, *Engineering Failure Analysis* 45, pp. 106-117, 2014.
- [7] Vishay Micro-Measurements. PhotoStress® Instruments, [Online], Available: http://www.vishaypg.com/docs/11212/11212_tn.pdf [28.04.2019], 2019.
- [8] ASTM E 837-13a: Standard Test Method for Determining Residual Stresses by the Hole-Drilling Strain-Gage Method, [Online], Available: <https://www.astm.org/Standards/E837.htm>, [05.02.2019], 2019.
- [9] ERRAPART, A., ANTON, J.: *Photoelastic residual stress measurement in nonaxisymmetric glass containers*, EPJ Web of Conferences 6, 32008, 2010.
- [10] SCHAJER, G. S.: *Practical residual stress measurement methods*, John Wiley & Sons Ltd, The Atrium, Southern Gate, Chichester, West Sussex, PO19 8SQ, United Kingdom, 2013.
- [11] NELSON, D.V.: Residual Stress Determination by Hole Drilling Combined with Optical Methods, *Experimental Mechanics*, Vol. 50, No. 2, pp. 145-158, 2010. doi:10.1007/s11340-009-9329-3
- [12] HARRINGTON, J.S., SCHAJER, G.S.: Measurement of Structural Stresses by Hole-Drilling and DIC, *Experimental Mechanics*, Vol. 57, No. 4, pp. 559-567, 2017.
- [13] TREBUŇA, F., PÁSTOR, M., HUŇADY, R., FRANKOVSKÝ, P., HAGARA, M.: *Optické metódy v mechanike*, Košice, TUKE, pp. 550, 2017. (Original in Slovak)

EVALUATION OF RESIDUAL STRESSES USING OPTICAL METHODS

Ján Kostka; Peter Frankovský; Peter Čarák; Vojtech Neumann

- [14] VEQTER, [Online], Available: <http://www.veqter.co.uk/residual-stress-measurement/centre-hole-drilling> [15.05.2019], 2019.
- [15] KOSTKA, J., PÁSTOR, M., ČARÁK, P., FRANKOVSKÝ, P., KULA, T.: *Návrh metodiky zisťovania zvyškových a prevádzkových napätí odvrávaním drážky pomocou dutej frézy*, Novus Scientia 2017, Košice, TUKE, pp. 88-92, 2017. (Original in Slovak)
- [16] KOSTKA, J.: *Využitie optických metód experimentálnej mechaniky pri analýze príčin porúch nosných prvkov konštrukcií*, Dissertation thesis, Košice, 2018. (Original in Slovak)
- [17] NELSON, D. V.: Residual stress determination by hole drilling combined with optical methods, *Experimental Mechanics*, Vol. 50, No. 2, pp. 145-158, 2010.
- [18] SCHAJER, G. S.: Advances in hole-drilling residual stress measurements, *Experimental mechanics*, Vol. 50, No. 2, pp. 159-168, 2010.
- [19] SCHAJER, G. S.: Relaxation methods for measuring residual stresses: techniques and opportunities, *Experimental Mechanics*, Vol. 50, No. 8, pp. 1117-1127, 2010.
- [20] VOURNA, P., KTEA, A., TSAKIRIDIS, P. E., HRISTOFOROU, E.: *A novel approach of accurately evaluating residual stress and microstructure of welded electrical steels*, NDT & E International, 71, pp. 33-42, 2015.
- [21] BANIARI, V., BLATNICKÁ, M., ŠAJGALÍK, M., VAŠKO, M., SÁGA, M.: Measurement and numerical analyses of residual stress distribution near weld joint, *Procedia engineering*, 192, pp. 22-27, 2017.

Review process

Single-blind peer review process.



JOURNAL STATEMENT

Journal name:	Acta Mechatronica
Abbreviated key title:	Acta Mechatron
Journal title initials:	AM
Journal doi:	10.22306/am
ISSN:	2453-7306
Start year:	2016
The first publishing:	March 2016
Issue publishing:	Quarterly
Publishing form:	On-line electronic publishing
Availability of articles:	Open Access Journal
Journal license:	CC BY-NC
Publication ethics:	COPE, ELSEVIER Publishing Ethics
Plagiarism check:	Worldwide originality control system
Peer review process:	Single-blind review at least two reviewers
Language:	English
Journal e-mail:	info@actamechatronica.eu

The journal focuses mainly on original, interesting, new and quality, theoretical, practical and application-oriented contributions to the scientific fields and research as well as to pedagogy and training in mechatronics.

Publisher:	4S go, s.r.o.
Address:	Semsa 24, 044 21 Semsa, Slovak Republic, EU
Phone:	+421 948 366 110
Publisher e-mail:	info@4sgo.eu

**Responsibility for the content of a manuscript rests upon the authors
and not upon the editors or the publisher.**